KTH Industrial Engineering
and Management

Parallel CO2 refrigeration system compared to state-of-the-art solution in supermarket application

David Garcia Redondo

Tutor: Samer Sawalha

Master of Science Thesis
KTH School of Industrial Engineering and Management
Energy Technology EGI-TRITA-ITM-EX 2019-563
Division of Applied Thermodynamics and Refrigeration
SE-100 44 STOCKHOLM

KTH Industrial Engineering and Management

Master of Science Thesis EGI
TRITA-ITM-EX 2019:563

The next generation energy systems for supermarkets

David Garcia Redondo

Approved	Examiner Samer Sawalha	Supervisor Samer Sawalha
	Commissioner	Contact person

Abstract

This thesis compares the performance of two trans-critical CO2 refrigeration systems, the state-of-the-art booster system and the standard parallel system. The main goal is to quantify the efficiency difference between these two systems.

By using computer assisted calculations both systems are modelled, then energy results are obtained. Different configurations for the parallel solution are considered. Adding direct expansion sub-cooling or using indirect sub-cooling, gives a significant improvement in the performance of the system. Also, a heat recovery control system is considered to operate when a heat load is demanded.

The calculations indicate that standard parallel system with the assumptions given, become a more efficient solution with a COP of 6,8 and 3 for the MT level and LT level respectively. This translate in energy saving of 9% and 7,6% when the heat recovery control system is used in comparison with the state-of-the-art booster system.

Acknowledgements

I would like to express my very great appreciation to my supervisor for all the help given in the making of this thesis. To all my colleagues who have been working side by side with me. To my family who have always supported me.

Thank to you all.

David Garcia Redondo

Stockholm, June 2019

Index

Nomenclature

CD	Cooling demand
CO2	Carbon dioxide
COP	Coefficient of performance
DH	District heating
DX	Direct expansion
ECU	Expander-Compressor-Unit
GWP	Global warming potential
HD	Heat demand
HFC	Hydrofluorocarbons
LT	Low temperature level
LWT	Low water temperature
MT	Medium temperature level
Ref	Refrigeration/refrigerant
SotA	State-of-the-Art

Variables

$\dot{E}$	Electric power, kW
h	Enthalpy per unit mass, kJ kg^{-1}
$\dot{m}$	Mass flow rate, kg s^{-1}
P	Pressure
PR	Pressure ratio
$\dot{Q}$	Cooling or heating load, kW
T	Temperature
Δ	Difference
η	Efficiency

Subscripts

amb	Ambient
comp	Compressor
gc	Gas cooler

HR	Heat recovery
is	Isentropic
LT	Low temperature level
max	Maximum
MT	Medium temperature level
o	Output
opt	Optimal
ref	Refrigeration/refrigerant
tot	Total

Index of figures

Index of tables

1 Introduction

Supermarkets are the industry which most contributes in Europe to the usage and production of high-GWP refrigerants, and one of the largest consumers of annual specific energy in the commercial designed buildings Sawalha et al. (2017). Also, the highest share of energy consumed belongs to refrigeration with a 47% of the total energy consumed, the share for lighting is 27%, for climate and fans control 13% and 13% for other uses Marimón et al. (2011) as shown in **Fig. 1**. Because of these reasons, changes implemented in supermarket's refrigeration systems can produce great reduction of the energy consumption and a potential improvement in the usage of refrigerants in terms of sustainability and efficiency.

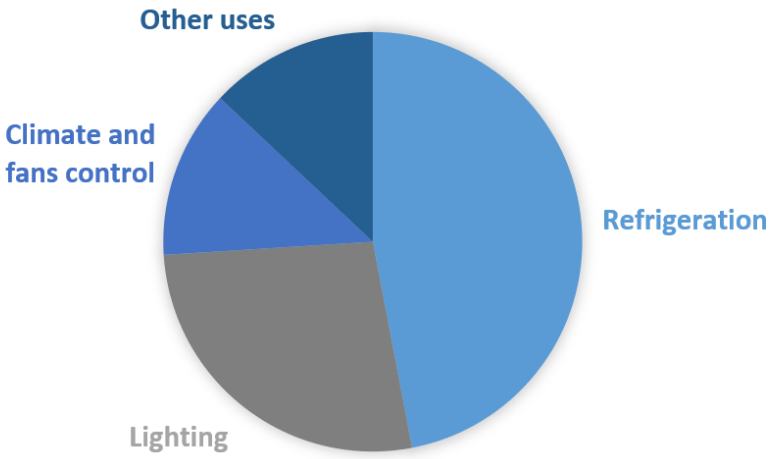

Fig. 1 Energy share in supermarkets.

The alarming global ecological crisis pushes technology to come up with environmentally friendly and energy efficient solutions for the industries. Therefore, a shift in the refrigeration systems for supermarkets towards sustainability and efficiency will represent the future of this industry.

The last revision of the Montreal Protocol by United Nations in Kigali (2016), stated that all parties must reduce gradually its HFC use by 80-85% by late 2040s UNEP (2016). This regulation can be found in the Kigali Amendment where focus is made in HFC´s global warming potential and how it must be cut down to achieve the goal of avoiding the 0.5 ºC potential rise of global temperature due to these substances. A summary of the evolution of the reduction in the usage of HFC refrigerants is shown in **Fig. 2**, where a 79% reduction is expected by 2030 taking 2010 as reference SuperSmart (2016). This evolution trend explains why conventional HFC based solutions are not feasible for a long-term perspective.

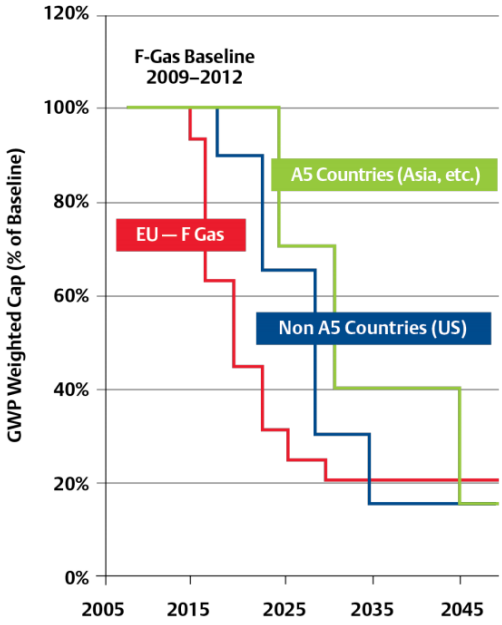

Service and maintenance bans	GWP	Timing
HFC's	2,500	Jan. 2020
'Placing on the market' (new equipment) bans		
Domestic refrigerators and freezers	150	Jan. 2015
Refrigerators and freezers for commercial use (hermetically sealed systems)	2,500	Jan. 2020
Refrigerators and freezers for commercial use (hermetically sealed systems)	150	Jan. 2022
Stationary refrigeration equipment (except equipment for temperatures below -50 °C)	2,500	Jan. 2020
Multipack centralized refrigeration systems for commercial use with a capacity of ≥ 40 kW (140 kBTU/hr) (except in the primary refrigerant circuit of cascade systems, where fluorinated greenhouse gases with a GWP of less than 1,500 may be used)	150	Jan. 2022
Movable room air-conditioning appliances (hermetically sealed equipment which is movable between rooms by the end user)	150	Jan. 2020
Single split air-conditioning systems containing < 3 kg	770	Jan. 2025

Fig. 2 Evolution of the usage of HFC refrigerants SuperSmart (2016).

Therefore, sustainable changes for refrigeration systems have to been made. It can be considered that supermarkets have three options to adapt to this regulation SuperSmart (2016).

- Keep using HFC refrigerants until 2020, and then use reclaimed or recycled gases until 2030. This operation decision would imply stricter requirements, near future ban and higher price and lower availability of refrigerants and equipment.

- Convert or adapt existing systems to prepare them to operate using synthetic refrigerant with lower GWP. This solution would satisfy the actual legislation, but there is a risk that future regulations would also ban these synthetic refrigerants in the same way that CFCs (Chlorofluorocarbons) and HCFC (hydrochlorofluorocarbons) have been prohibited.

- To replace the actuals system by ones using natural refrigerants with no GWP. Even though in the past this type of systems weren't the most feasible solution, innovations have led this technology towards a competitive position in the refrigeration market. For instance, investment costs in North-Centre Europe are no longer higher than conventional solutions for refrigeration. Also, in warm countries the operation cost has decreased enough to even produce savings.

For the reasons explained above, the future for supermarkets refrigeration systems is declining towards a natural-refrigeration system operation. This Master thesis studies the potential of CO2 as a replacement for conventional refrigerants and how can be improved to be more efficient.

2 Objectives

The aim for this Master thesis is to evaluate the efficiency of CO2 refrigeration systems for supermarkets. This study relies in the comparison between two systems, one is a parallel system using CO2 as refrigerant, and the other is the state-of-the-art system introduced by Karampour & Sawalha (2018). The standard system is studied in three different configurations to give a better understanding of the efficiency potential of this system. Firstly, an uncoupled arrangement is presented as the base line of the study, then a sub-cooling unit is introduced, and finally, a secondary loop with a brine is considered for achieving the sub-cooling on the evaporators. Furthermore, a control system to recover heat introduced by Karampour and Sawalha (2018) for the booster system, is implemented for the standard system to make an accurate comparison.

The systems analysed uses CO2 as a refrigerant which has been subject to extensive research in the past years. Today, modern supermarkets use a single integrated energy system to provide all thermal needs.

This project runs in parallel to a research project for one of the largest supermarket's companies in Sweden, with the aim of building the most efficient supermarket of today. In order to fulfil this project, ten industrial partners are working together studying the proposed design of state-of-the-art CO2 system in order to build the system and analyse it via field measurements and modelling.

3 Methodology

To reach a solution for the problem presented, the following methodology is being used. Firstly, to model the refrigeration system, data is collected from previous work on CO2 refrigeration systems by Karampour & Sawalha (2018). The boundary conditions and assumptions are determined by this information, selecting them to match the conditions of the booster refrigeration system, with the target of comparing the parallel and the SotA systems. Once the model is completed using advanced thermodynamics calculation software, further calculations such as energy efficiency, annual energy use, and savings are performed. Other modifications and possible improvements which potentially could result in higher energy efficiency are proposed. Finally, economical study and conclusions are presented.

3.1 Boundary conditions and assumptions

To reach the goal of this project, boundary conditions must be set thoroughly, in this manner the results for the analysed system and the booster system can be compared. For the rest of this section this information is presented. These assumptions are taken locating the system in Stockholm, Sweden, but the way this model is created, it can be implemented in any country of interest, just adapting the ambient temperatures to the new region all the calculation will adapt to the region conditions.

Supermarkets energy usage mainly stands in the refrigeration needs, this includes freezers and refrigeration cabinets located in the sales area. For this reason, these are the first conditions that are considered.

To storage safely the food products, temperatures of +3 ºC and -18 ºC are needed for the refrigeration and freezer cabinets respectively. To reach these temperatures, the evaporators temperatures are typically set to -8ºC and -32ºC for the MT and LT levels, with an external superheat of 10 K Karampour & Sawalha (2018).

The load for these components is determined by the following assumption. Typically, in supermarkets, refrigeration cabinets are open to the sales area, making them strongly depend on the ambient temperature. When the outdoor temperatures rise, humidity content in the ambient becomes higher resulting in an increase in the indoor humidity. Load in these cabinets follows the ambient temperature pattern, being 200 kW at 35 ºC and decreasing to 100 kW at 10 ºC and it is considered to remain constant at this point for lower temperatures. Meanwhile, the load for the LT is assumed to be constant during the year because freezing units are covered by lids that prevent noticeable fluctuations in the temperature. The cooling load for these is set to be 30 kW while the system is operating. Plots of the profiles for heating and cooling demand are shown in **Fig. 3** Karampour & Sawalha (2018).

Heating demand for supermarkets can be reduced to space heating, neglecting domestic hot water demand because it is typically low in supermarkets. Space heating is assumed to be needed when ambient temperatures drops below 10 ºC. At this temperature the heating demand is 40 kW and increases linearly to 190 kW for the lowest temperature studied of -20 ºC. The evolution of the different loads versus the ambient temperature it is represented in the **Fig. 3** Karampour & Sawalha (2018).

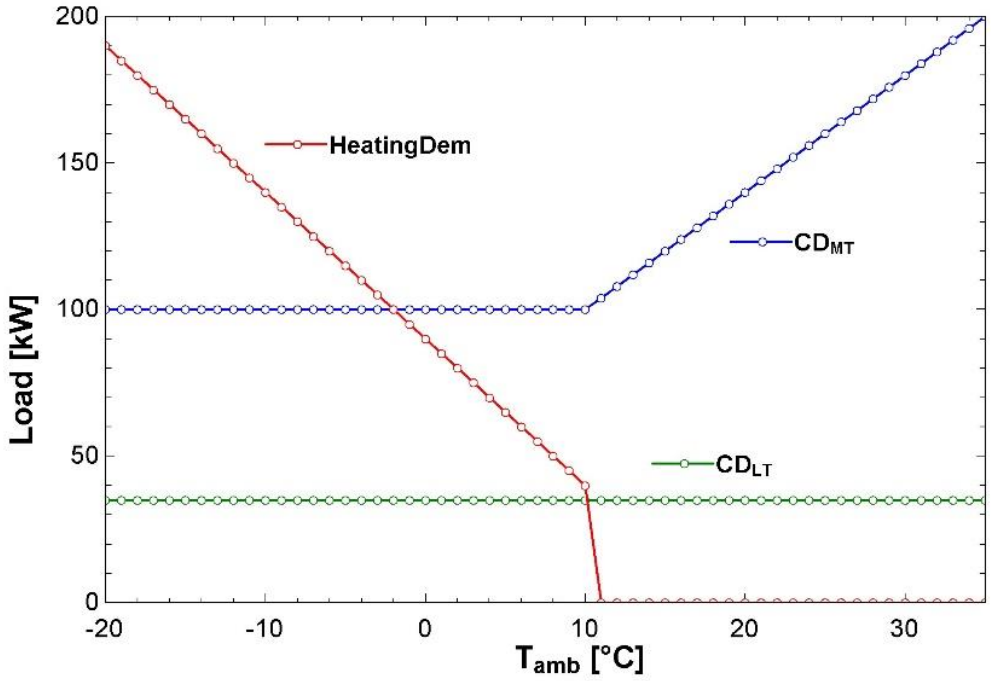

Fig. 3 Cooling and heating loads profiles Karampour & Sawalha (2018).

3.2 Systems model

3.2.1 System solutions

Three main system solutions are analysed to study how different variations in the basic model affects the efficiency of the cycles. Firstly, a system with a heat-exchanger is presented, interconnecting MT and LT cycles to increase the sub-cooling in the LT gas cooler exit. The next system solution relies in a secondary loop, also with the same porpoise of sub-cooling the LT line after the gas cooler but indirectly. Finally, the system is studied with both, LT and MT, totally uncoupled to analyse the result of not using any efficiency measure and how this affects the total energy use of the system. Schematics of the systems in the three solutions will be presented in the following sections.

3.2.1.1 System solutions with direct sub-cooler

This first system is composed of two different loops to feed the thermal loads required in the cooling units. LT loop supplies to the freezers and the MT one the refrigerating cabinets. This system is characterized by the sub-cooling unit that links both loops, as can be seen in **Fig. 4**, increasing the enthalpy difference in the LT evaporator, enlarging its cooling capacity. The minimum temperature reachable for the refrigerant in the MT level evaporator is -3 ºC. The P-h diagram that this solution describes is plotted in **Fig. 5**.

As can be seen in **Fig. 4**, MT level has a secondary line, bypassing the evaporator, to feed the sub-cooler. Doing this it is possible to control the heat that is exchanged between both cycles variating the mass flow that runs through the heat exchanger.

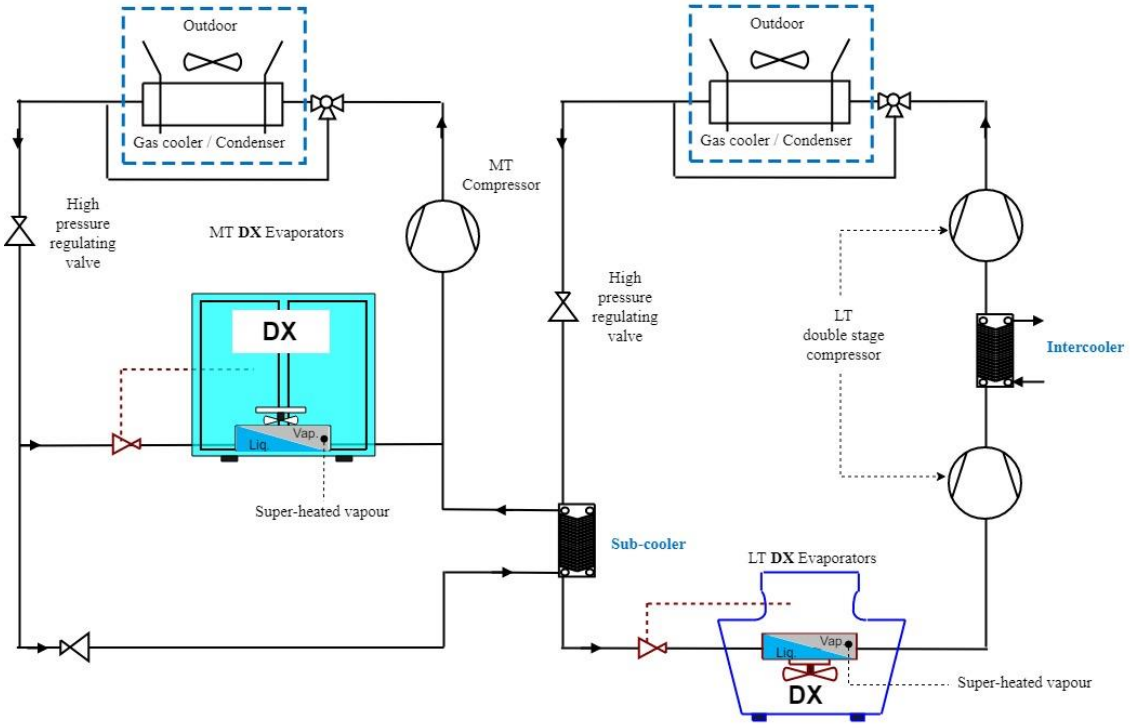

Fig. 4 Diagram of the direct sub-cooling solution for parallel system.

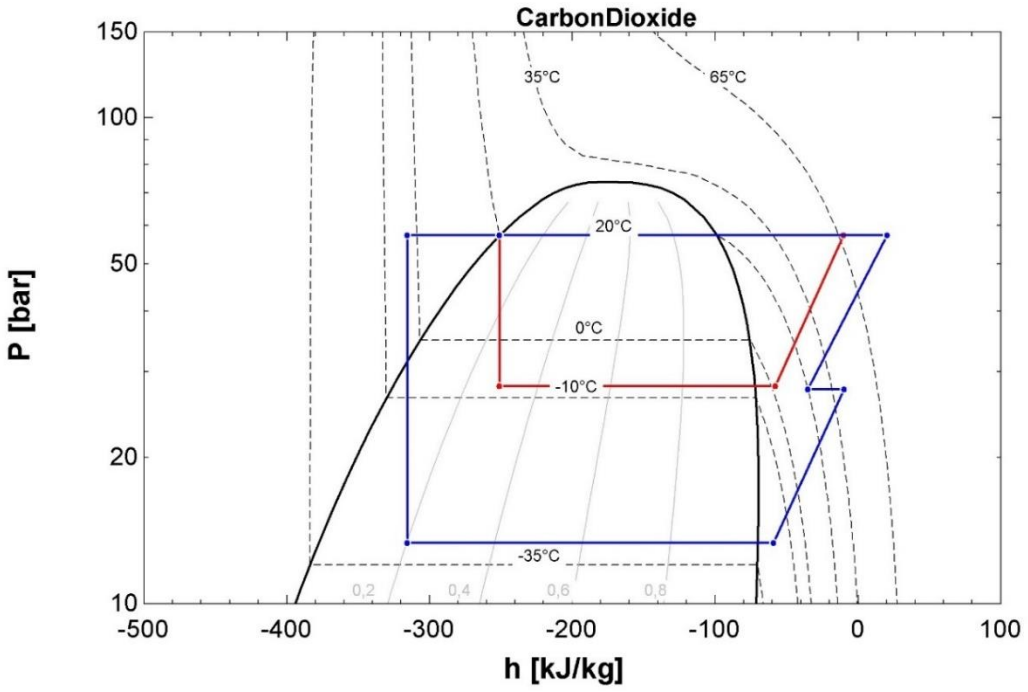

Fig. 5 P-h diagram for the sub-cooling solution.

3.2.1.2 System solution with indirect sub-cooler; i.e. brine loop

In this solution, instead of using a direct expansion heat exchanger to transfer heat from the LT loop to the MT one, a secondary cycle, for example a brine cycle, is chosen for this task **Fig. 6**. Is important to mention that for simplicity non particular brine has been specified, because it is not required for solving the equation system generated in this secondary loop.

The main advantage for using this arrangement is the ease in the control system. Due to derivate the sub-cooling procedure to a secondary cycle with own mass flow, reduces the parameters to control in the primary cycles, also giving more stability in the fluctuation of temperatures. Control on this type of cycles is one of the most challenging issues, and easing this task makes it simpler to operate in exchange of losing efficiency.

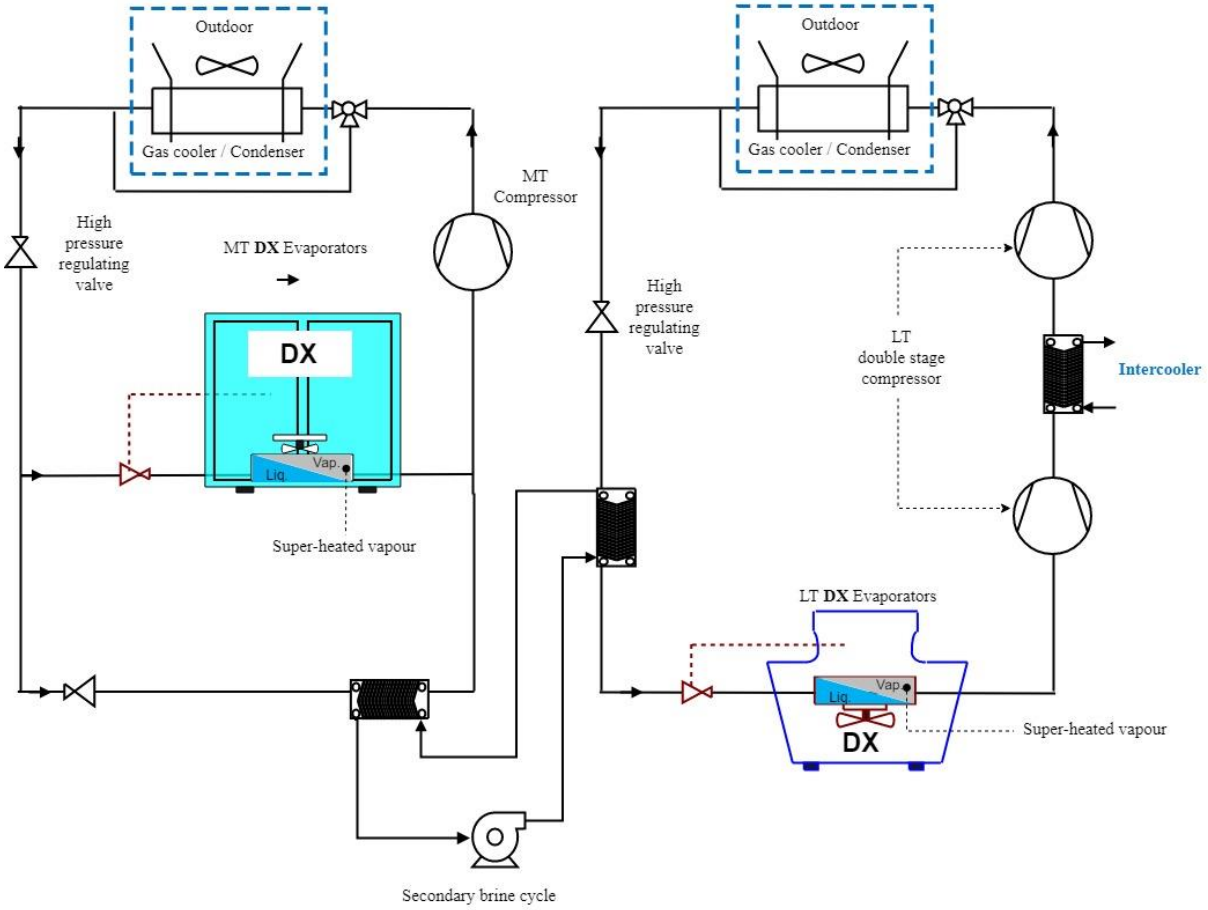

Fig. 6 Diagram of the indirect sub-cooling solution for parallel system.

After the refrigerant exits the MT gas cooler, it divides its mass flow into two different lines. One pass through the expansion valve and then through the MT evaporator, while the other flow bypasses the MT evaporator to expand in a different valve and then uses its cooling capacity to absorb heat from the brine solution in the heat exchanger, shown in **Fig. 7** (top). For this type of secondary cycles a thermal approach (dT) of 2 K is estimated. After this, the now cooled brine flows to the LT heat exchanger, sub-cooling the gas/liquid at the exit of the gas cooler/condenser

that will expand afterwards. In **Fig. 7** the temperature profile is shown using references to the connections between the MT and LT levels with the brine loop.

Finally, as can be seen in **Fig. 8** and compared to **Fig. 5**, the P-h diagram is similar to the one obtained from the sub-cooling system. Due to the short length of the secondary loop, the pressure drop is neglectable.

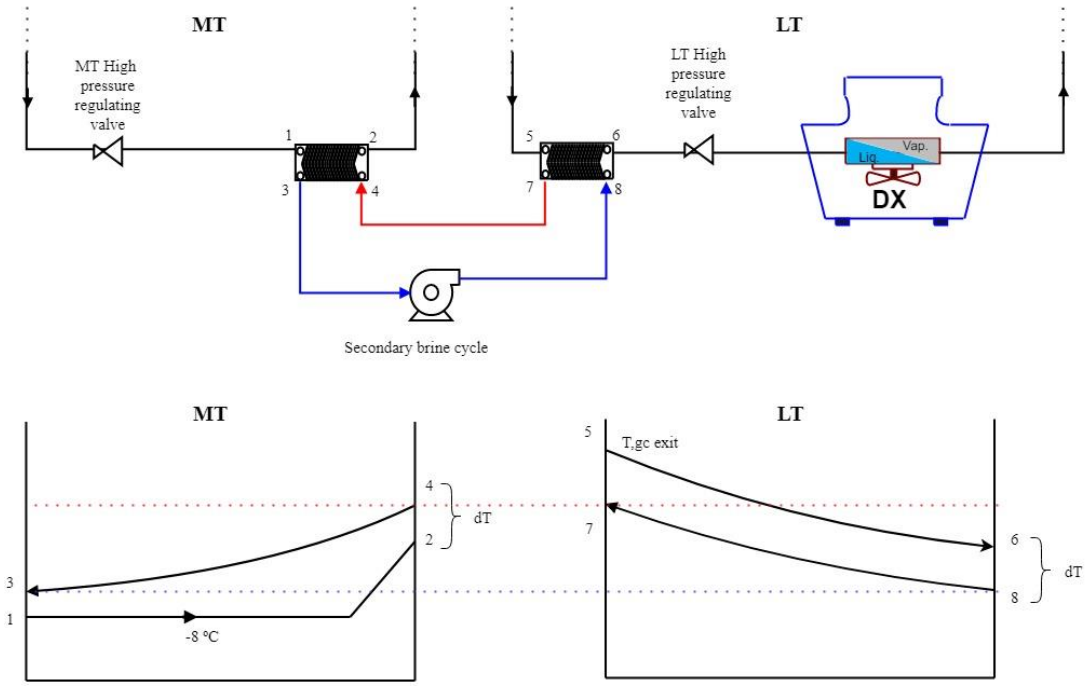

Fig. 7 Detailed diagram of the indirect sub-cooling solution for the parallel solution (top) and thermal profiles for the inlets and outlets of the heat exchangers (bottom).

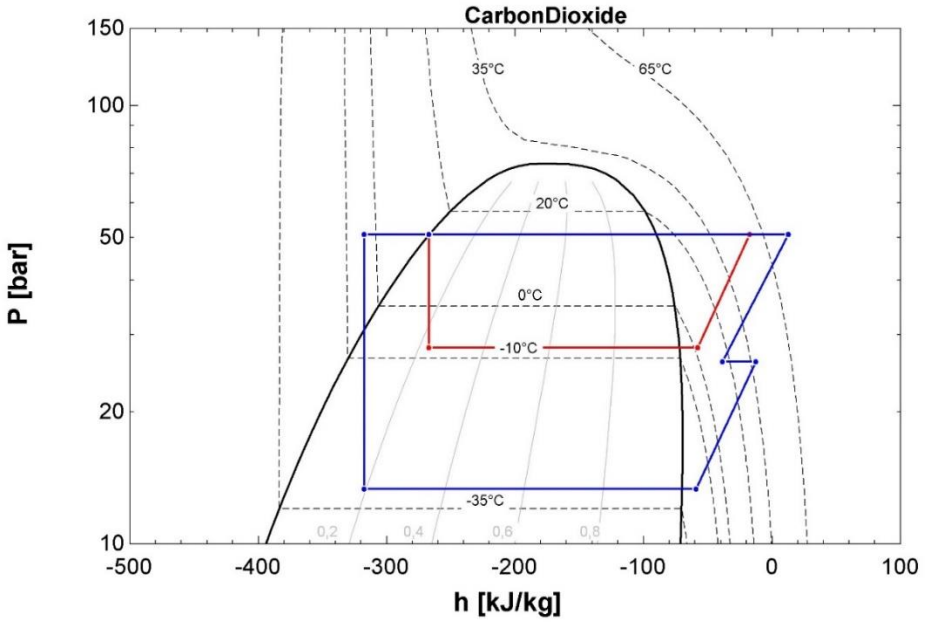

Fig. 8 P-h diagram for the indirect sub-cooling solution.

3.2.1.3 Parallel uncoupled

Thirdly, this arrangement is used to study the solution where no sub-cooling is used. MT and LT level are uncoupled, meaning that there is no heat transferred from on loop to the other as can be seen in **Fig. 9**. This solution eases the control task, simplifying the mass flow removing the bypass for the sub-cooler unit used in the other solutions. As a result of this, the gas in the gas cooler output is in saturation, as shown in **Fig. 10**. Having a narrower enthalpy difference in the evaporators in comparison to the other two solutions.

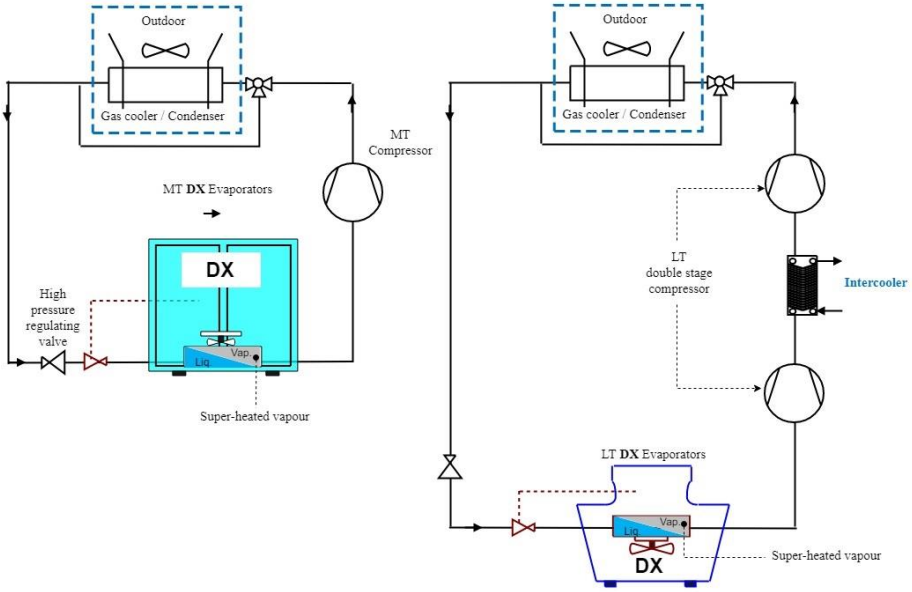

Fig. 9 Diagram of the parallel uncoupled solution.

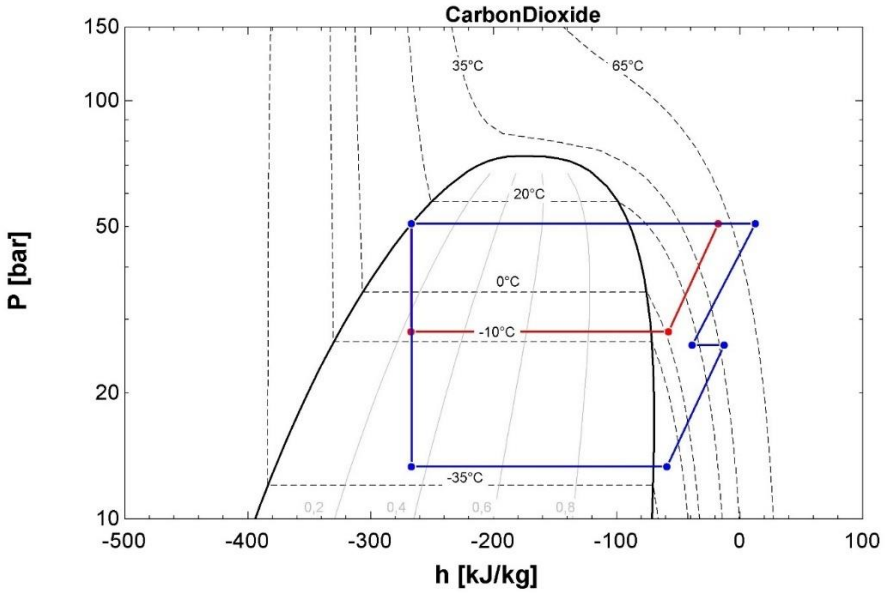

Fig. 10 P-h diagram for the uncoupled solution.

3.2.2 Compressor

For the MT level a single stage compressor is selected, given the similarity of operation, the efficiency curve for the compressor used in the booster introduced by Karampour and Sawalha (2018). This compression curve follows the Eq.(1).

$$\eta_{MT} = \frac{-2.7854\left[\frac{P_{gc}}{P_{evap,MT}}\right]^2 + 19.477\frac{P_{gc}}{P_{evap,MT}} + 33.013}{100} \ [\%] \quad (1)$$

On the other hand, LT level double stage compressor is selected from Dorin catalogue. Using the chart shown in **Fig. 11**, and knowing the volumetric flow at the entrance of the compressor, the compressor range can be determined. With a volumetric flow of 15.22 m3/h the range needed is determined to be CD2S-400. Afterwards using the software that the compressor manufacturer provides, model CD2S1200 is selected.

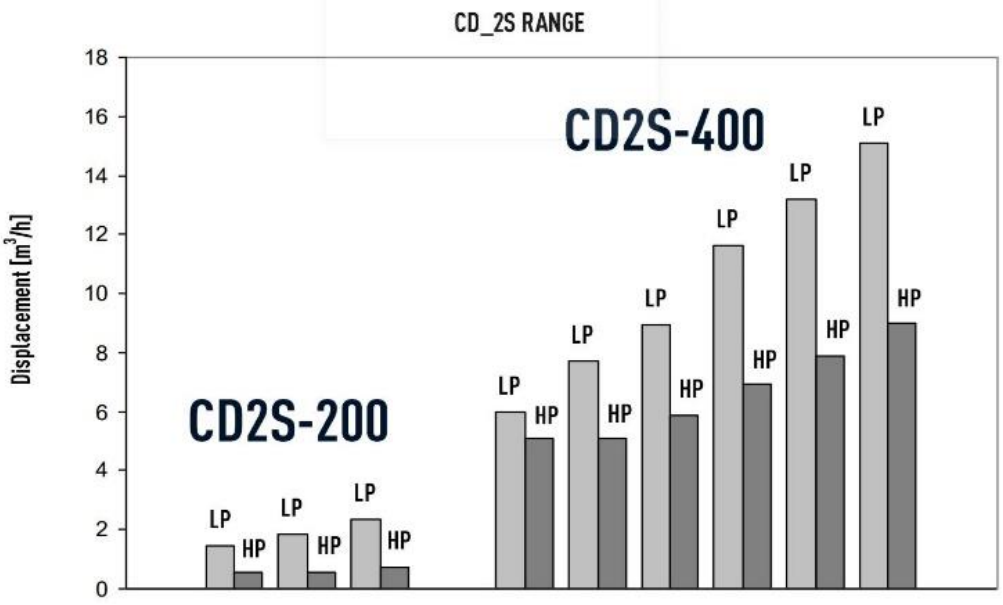

Fig. 11 Compressors range vs volumetric flow displacement Accessori et al. n.d..

The relation between the total efficiency and the pressure ratio for different working conditions was calculated using Dorin software, variating the discharge pressure and evaporation temperature. These conditions include situations where the equipment work in subcritical and transcritical operation modes. The second boundary condition is the temperature reached in the intercooler between both stages of the compression. This temperature is assumed to be the same as the gas cooler's exit temperature, because the intercooler rejects heat to the same heat sink. With this calculations, the chart shown in **Fig. 12** is generated, and the efficiency curve calculated Eq.(2).

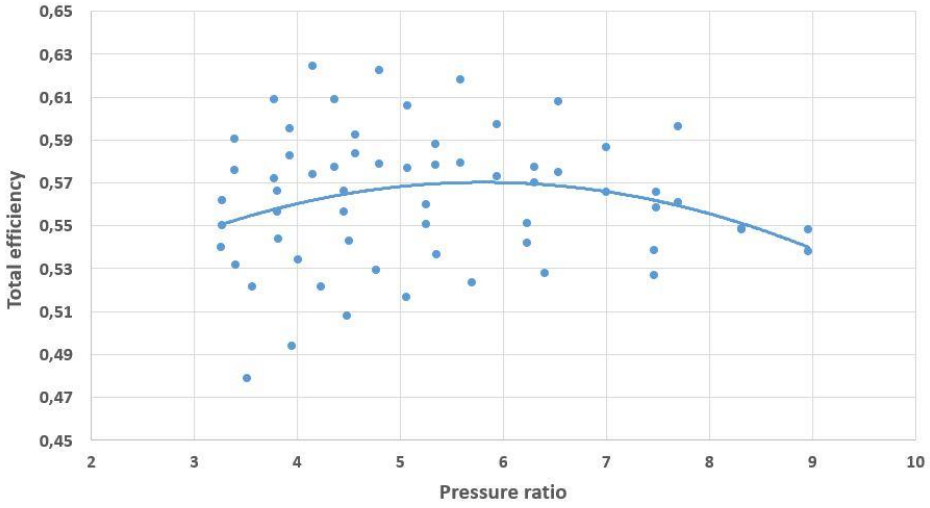

Fig. 12 Performance curve for Dorin compressor CD2S1200, comparing efficiency versus Pressure ratio.

$$\eta_{LT} = -0.003\left[\frac{P_{gc}}{P_{evap,LT}}\right]^2 + 0.354\frac{p_{gc}}{P_{evap,LT}} + 0.4676\ [\%] \quad (2)$$

Further studies are performed thanks to the wide range of options given by Doring software, such as calculating efficiencies for diverse set up of compressors. For example, using two separated compressors for each of the stages of the compression. Because its higher efficiency, the semi-hermetic double stage compressor is selected.

Calculations are done for two different possibilities, one studying the efficiency for one double staged compressor, and second for a set with two single stage compressors configurated in series. Finally, in the energy efficiency calculation, section 3.4, this choice will be justified by the energy consumption ratios for the two main studied sets of compressors.

3.2.3 Gas cooler

The MT and LT gas coolers and the intercooler for the compressor are connected to outdoors extracting the heat from the system outdoors. The temperature approach (dT [K]) between ambient temperature (T_{amb} [ºC]) and the gas cooler exit ($T_{gc,o}$ [ºC]) is 7K Karampour & Sawalha (2018).

The control system sets the gas cooler operation condition to match the optimal discharge pressure ($P_{disch,op}$ [bar]) defined by the Eq.(3).

$$P_{opt} = 2.7\left(\mathrm{T_{amb}} + \mathrm{T}_{gc,app}\right) - 6.1\ [\mathrm{bar}] \quad (3)$$

3.2.4 Heat Recovery

Heat recovery system is designed to use rejected heat and re-use it, in this case, to heat the indoor sales area when is needed. To model it, the return temperature for the heat recovery system is assumed to be 30 ºC with a thermal approach of 5 K. Therefore, is possible to recover heat until the CO2 running in the MT cycle reaches 35 ºC, then to recover a higher heat quantity, pressure in the gas cooler has to be increased Karampour & Sawalha (2018).

The heat recovery device is only installed in the MT loop as shown in **Fig. 13**. this is due to LT level has a lower efficiency. Maintaining the LT condensing temperature as low as possible ensures to keep the efficiency with higher values. As the heat recovery control system makes the system to work in the transcritical region, would make the compressors to work with a higher pressure ratio and thus, decrease the overall efficiency.

The heat recovery control system based in the design by Sawalha (2012) is briefly introduced. When the outdoor temperature decreases below 10 ºC the heating system start working following the demand curve shown in **Fig. 3**. When this happens, the heat begins to be extracted from the MT loop, using a heat exchanger situated between the compressor and the gas cooler (Q_{HR}) as can be seen in **Fig. 13.** If the heat load is greater than the available in this setting, then the pressure of the MT gas cooler is risen. This occurs because the enthalpy difference between the compressor exit and the 35 ºC limit, is not wide enough, as can be noted in **Fig. 14**. Eq. (4) is used to calculate the heat recovered, knowing the mass flow that runs through the heat exchanger ($\dot{m}_{ref}$ [kg·s^{-1}]), and the enthalpy difference between the output point of the compressor, and the output enthalpy of the heat recovery heat exchanger, calculated knowing the pressure and temperature this point. This operation mode carries on until the maximum optimum discharge pressure ($P_{disch,opt,max}$) is reached, maintaining the exit temperature in the gas cooler at its minimum. This discharge pressure is calculate similarly as before, using Eq.(2), and using the exit temperature of the heat exchanger instead of the term (T_{amb}+$T_{gc.app}$).

At this point, if the heating demand is not satisfied, then the sub-cooling is turned down, and reduce the fan speed to increase the mass flow. Once the sub-cooling reaches to zero, then the maximum heat recovery capacity is reached, and producing heat cannot be increased without losing great amount of efficiency. Beyond this point it is no longer feasible to recover more heat.

$$\dot{Q}_{HR} = \dot{m}_{ref}\left(h_{compressor,exit} - h_{t=35\,ºC}\right) \text{ [kW]} \quad (4)$$

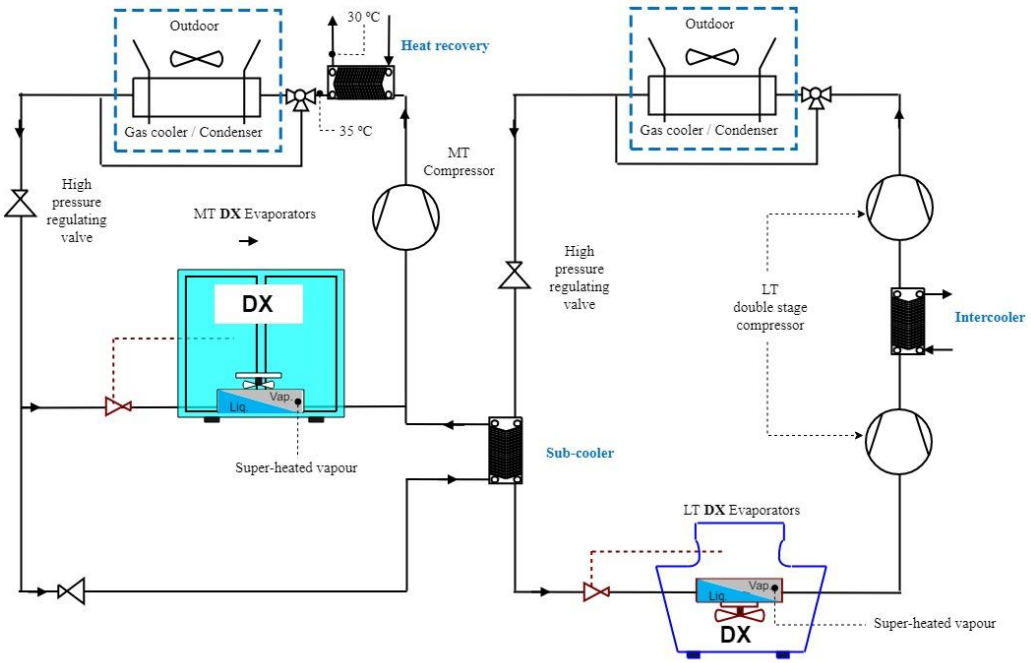

Fig. 13 Diagram of DX sub-cooling solution with the heat recovery unit in MT.

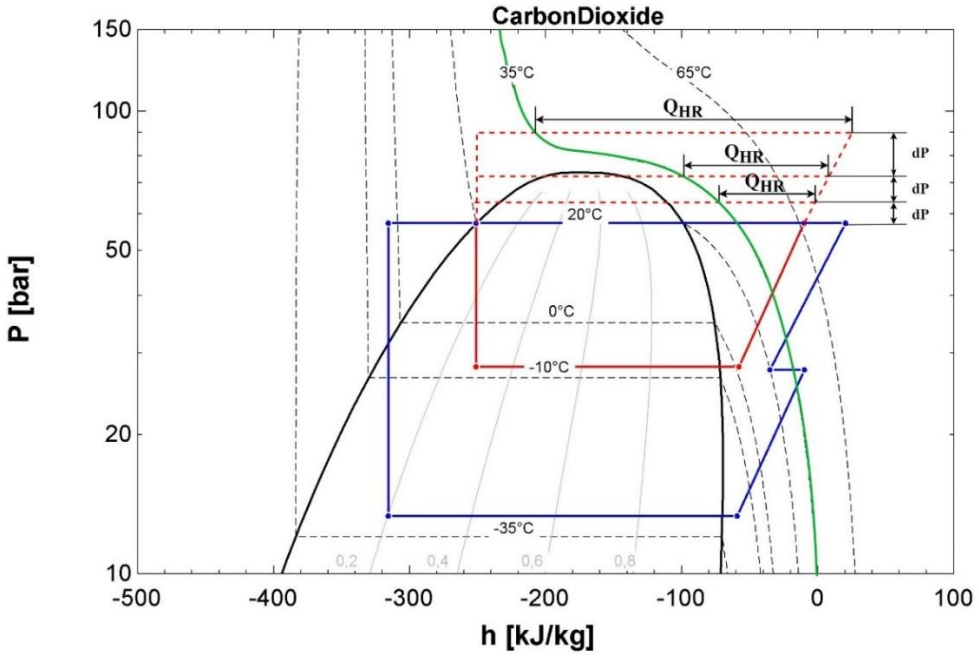

Fig. 14 P-h diagram for DX sub-cooling solution using heat recovery control system.

The system starts working when the ambient temperature is lower than 10°C, then the cycles will be driven to try to supply enough heat to match the heat demand. Even though the system is designed for refrigeration purpose, it is cheaper to produce extra heat in winter time and avoid using other methods Karampour & Sawalha (2018). This statement is justified by calculations in section 4.3.

3.3 State-of-the-art system

This system, modelled by Karampour & Sawalha (2018), is the base for the next part of the project. Once the previous cases are modelled, the study of this system is presented to subsequently compare them. The schematic for this system and its sample P-h diagram are shown in **Fig. 15** and **Fig. 16** respectively. This cycle is distinguished by the booster operation, having the lower and medium temperature levels linked. By doing this, the MT level compressor operates with the total mass flow of the system. Also, this compressor removes the vapor from the flash tank at a higher pressure level than at MT, which makes the system more efficient.

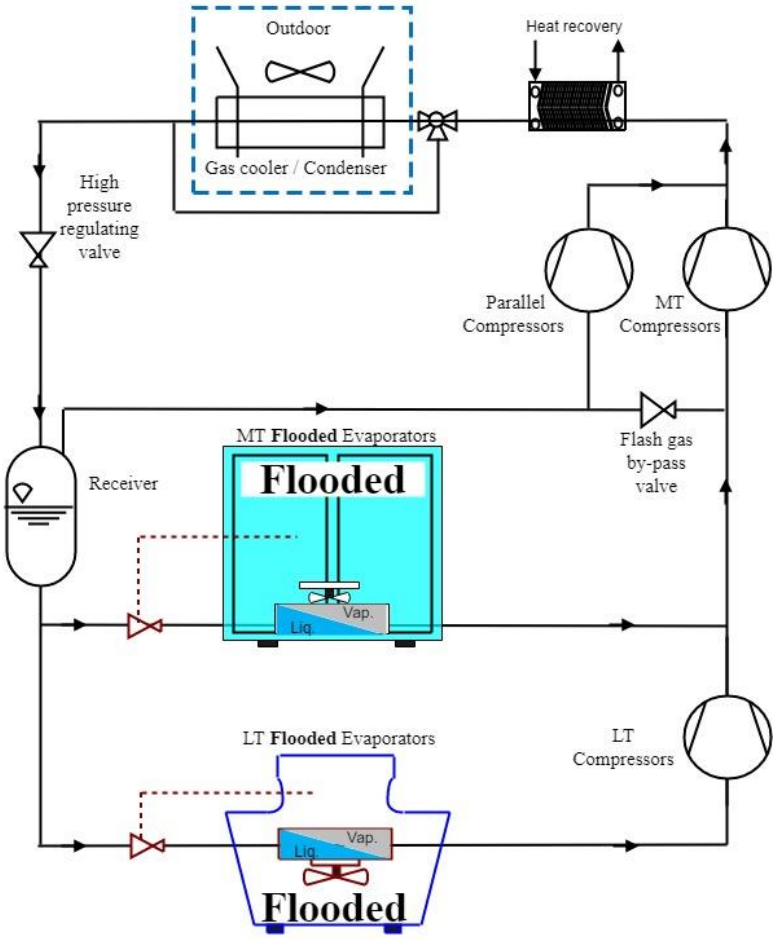

Fig. 15 Diagram of the state-of-the-art booster system Karampour and Sawalha (2018).

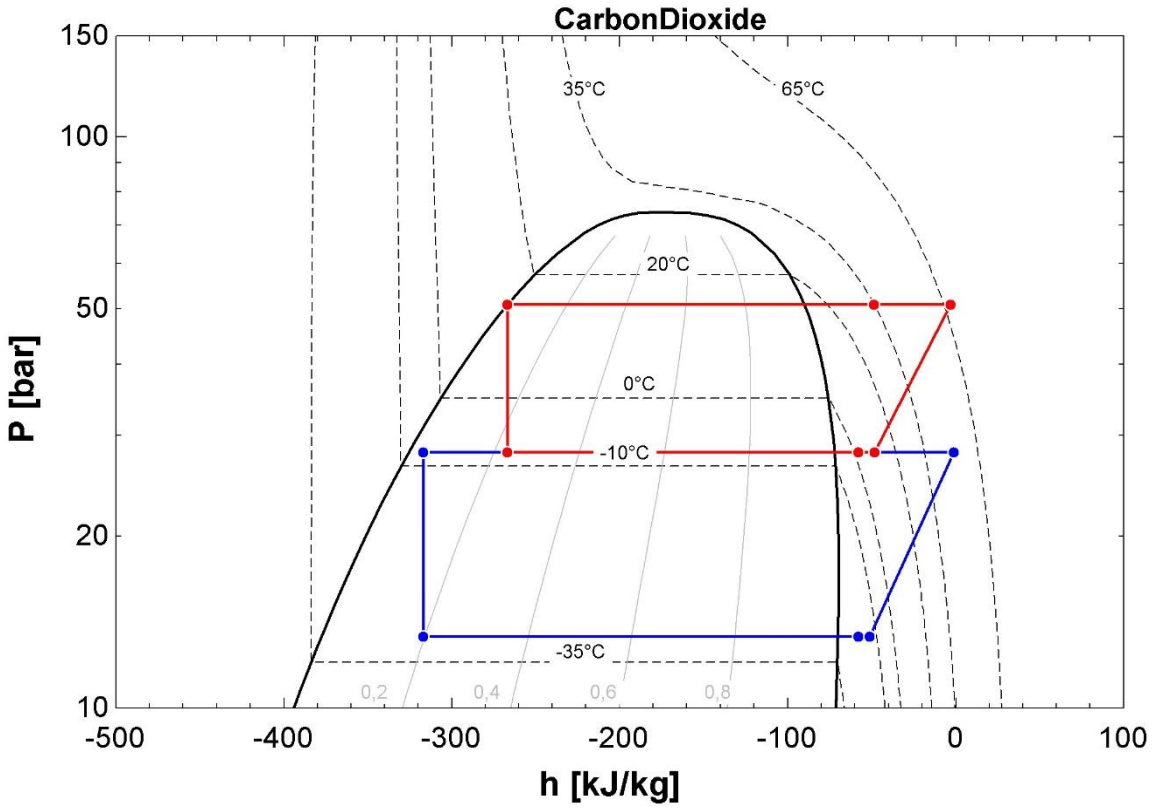

Fig. 16 P-h diagram for the state-of-the-art booster system.

3.4 Energy efficiency calculations

In this section calculations about the efficiency of each of the system solution are discussed. EES Klein (2015) is a software that offers high mathematical functions and being able to solve complex equations with its powerful calculus potential. The most important feature of this program regarding this project is the high accuracy thermodynamic property database which can be obtained by built in functions.

Firstly, mass flows are calculated using Eq. (5) and using the thermal loads as inputs $\dot{Q}$ [kW]. These inputs are the cooling demand for the refrigerating cabinets ($\dot{Q}_{MT}$) or for the freezers ($\dot{Q}_{LT}$). Depending on which load is studied, the enthalpy difference will be the one between the outlet and inlet on the evaporator. Therefore, $\dot{m}_{ref}$ [kg·s^{-1}] is the mass flow that runs through the evaporator.

$$\dot{Q} = \dot{m}_{ref} \cdot \Delta h_{heat\ exanger}\ [kW] \tag{5}$$

Consequently, the electric power consumed by the compressor is calculated with the same principle $\dot{E}_{comp}$ [kW]. Distinguishing between MT and LT compressor efficiency (η_{MT}) (η_{LT}) [%], the power can be calculated for each compressor separately using Eq. (6), being Δh_{is} [kJ·kg^{-1}] the enthalpy difference between the outlet and inlet of the compressor assuming an isentropic performance. In the case of MT level, as the mass flow varies depending on the system solution, Eq. (7) is used to add the mass flow that runs via the heat exchanger that feeds the sub-cooling system, or the secondary cycle with the brine.

$$\dot{E}_{comp} = \left(\dot{m}_{ref} \cdot \Delta h_{is}\right)/\eta_{tot}\ [kW] \tag{6}$$

$$\dot{m}_{ref} = \dot{m}_{MT} + \dot{m}_{sc}\ [\mathrm{kg \cdot s^{-1}}] \tag{7}$$

Once these parameters are calculated, COP is calculated for the different system solutions according to Eq. (8). Using the different inputs for each solution in Eq. (9) the total power consumption is calculated ($\dot{E}_{tot}$) [kW] for each case. Also, using Eq. (8) with the parameters for MT or LT level separately, makes possible compare the efficiency of the systems in overall or comparing each level specifically. The thermal power $\dot{Q}_{ref}$ can be determined to be equal to $\dot{Q}_{MT}$, $\dot{Q}_{LT}$ or $\dot{Q}_{tot} = \dot{Q}_{MT} + \dot{Q}_{LT}$ depending what is the subject of study (MT, LT or the whole system). The power consumption on the pump for the brine cycle system solution is considered neglectable given the fact that is a short loop and the pressure drop is insignificant ($\dot{E}_{pump,brine\_cycle}$) [kW].

$$COP_{ref} = \frac{\dot{Q}_{ref}}{\dot{E}_{tot}}\ [-] \tag{8}$$

$$\dot{E}_{tot} = \dot{E}_{comp,MT} + \dot{E}_{com,LT} + \dot{E}_{pump,brine\_cycle}\ [kW] \tag{9}$$

4 Results and discussion

In this section of the project results of the calculation of the model are discussed and presented. Thanks to this information, a formal comparison with accurate data is performed.

4.1 COP and Energy consumption

Firstly, the coefficient of performance (COP) is calculated taking as variable the ambient temperature and the results are plotted in **Fig. 17**. COP for the MT level in the parallel solutions are the same, with a value of 6.8 for the coldest temperatures of the year, even though the refrigeration load depends on the ambient temperature, because the power consumed by the compressors is directly proportional to the mass flow that has to process. The COP for the direct sub-cooling and for the indirect sub-coooling solutions in the LT level are almost equal, with a value over the 3 point mark, this is due to both have almost the same efficiency, being the indirect sub-cooling solution the one with a slightly lower sub-cooling capacity, due to the higher inlet temperature in the expansion valve. Finally, the uncoupled parallel system solution is the one with the lowest COP because of its lower cooling capacity in the LT evaporator, forcing the system to work with a higher mass flow to be able to produce the same amount of cooling. Booster system results are divided into MT and LT to compare it with the rest of the system solution.

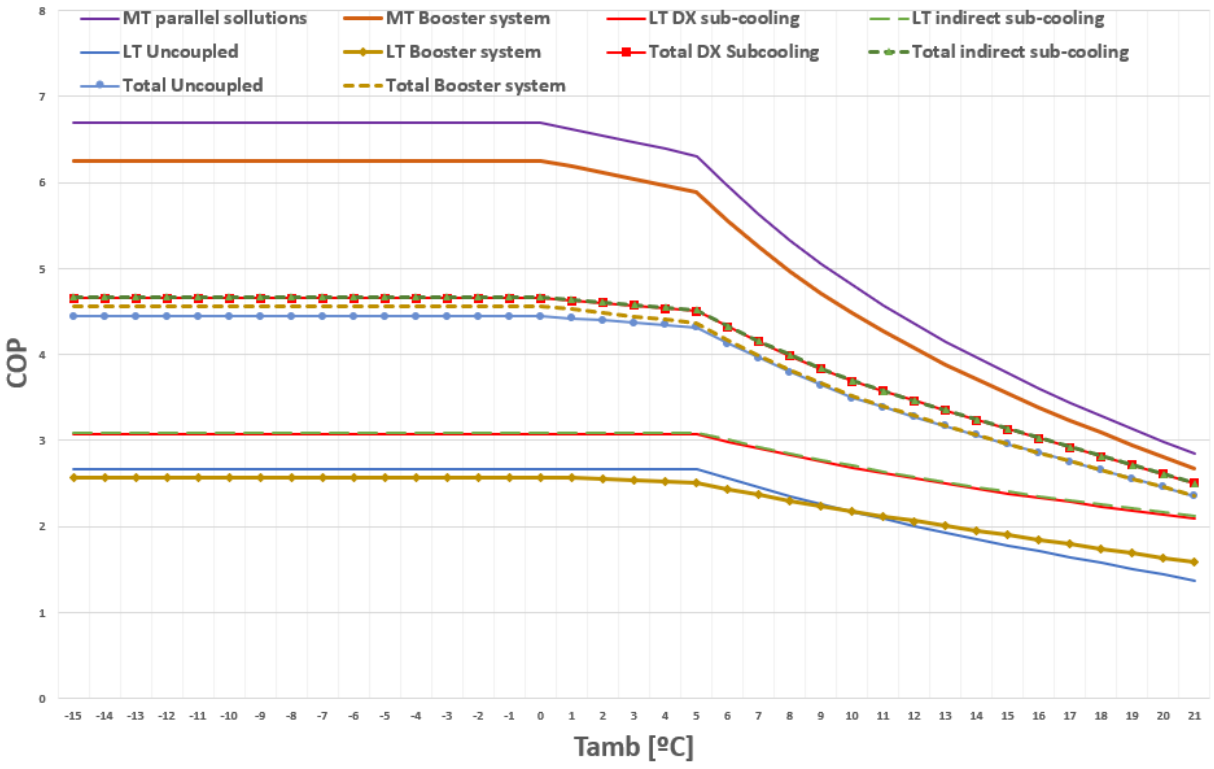

Fig. 17 Comparison graph for the different system solutions, COP vs Tamb.

After this, the total yearly energy consumption is calculated. The result of this is shown in **Fig. 18**, where the energy consumed is calculated using hourly data of the ambient temperature in Sweden throughout a year.

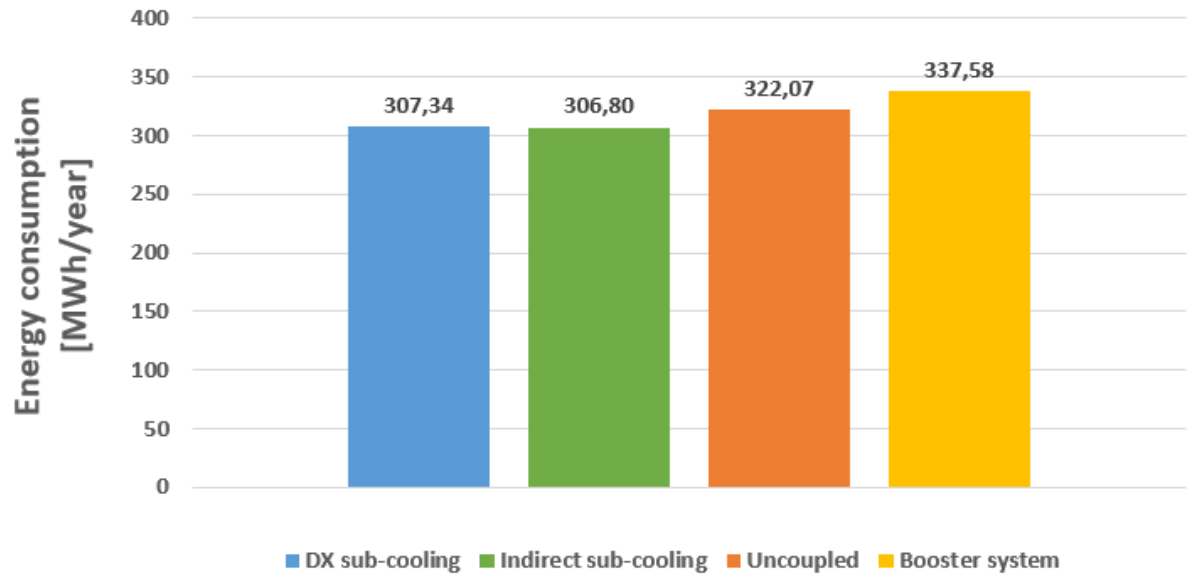

Fig. 18 Comparison chart of the energy consumption for the different system solutions [MWh/year].

Knowing this information, the percentage of energy savings is calculated taking as a reference the state-of-the-art booster system working with the same conditions as the three system solutions for the parallel system. As can be seen in **Fig. 19**, uncoupled system consumes the same amount as the booster system as it is expected. The savings for sub-cooling and brine cycle solutions are positive with an 8.96% and 9.12% yearly, that it translates to around 30 MWh saved per year.

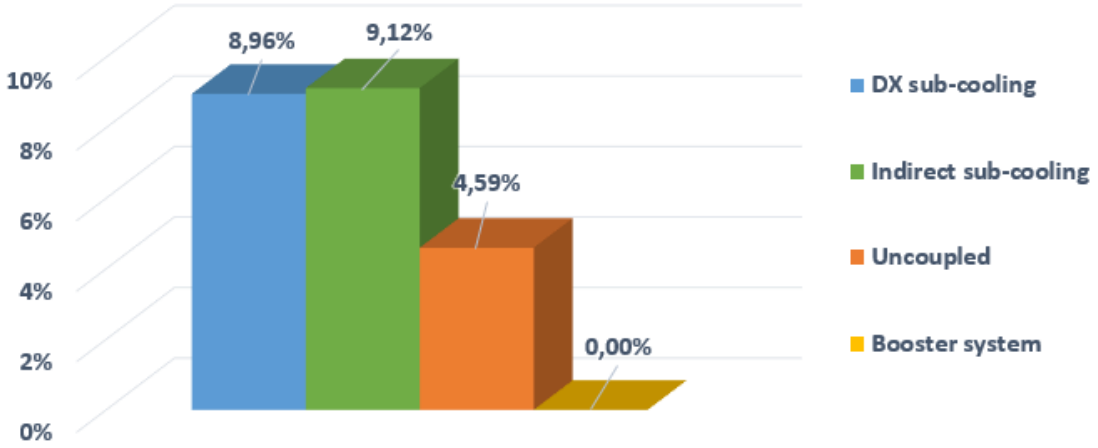

Fig. 19 Energy savings for parallel systems in percentage compared to state-of-the-art booster system [%].

After this first analysis, now heat recovery control is added to the model. In this solution it is expected that the energy consumption increases because the system is matching the cooling demand in winter mode, and once the ambient temperature decreases under 10 ºC, winter mode

activates and the system switches to match the heating demand. The results of this solution are presented below.

Fig. 20 shows the COP for the MT level in the three system solutions using the heat recovery control system. In blue, the value for MT without the heat recovery control system COP is represented for reference, showing the performance of the system in floating condensing mode. As expected, the COP drops significantly due to the greater load that has to be satisfied. Both, sub-cooling and using the secondary brine cycle results in an almost exact performance. In the other hand, the uncoupled configuration follows a similar pattern with performances around 0.1 and 0.2 lower in temperatures between -10 and 2 ºC.

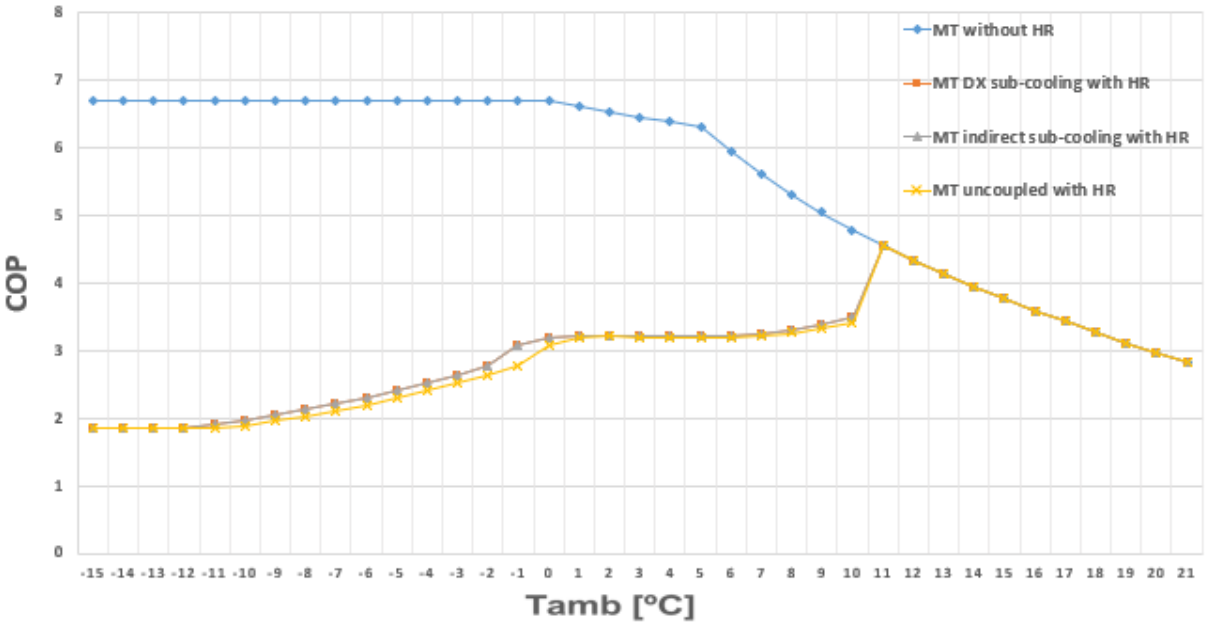

Fig. 20 Comparison graph for MT COP between the system solutions with heat recovery.

The results for the total COP with the heat recovery control system implemented are represented in **Fig. 21**. In this graph the total COP is shown, then a comparative analysis is performed. Using a sub-cooling approach or a secondary brine cycle to improve the cooling and heating capacity gives an almost exact result, making the decision to depend in other facts such control simplicity or robustness that depends on the client and emplacement of the project. Booster system has a better performance in the lowest ranger of temperatures, between -13 and -5 ºC, but it becomes less suitable in warmer conditions. Also, the response on the heating demand is quicker what makes the system have a less stiff COP curve along the temperature range. The uncoupled gives the worst performance, following the same pattern as the other two system solution.

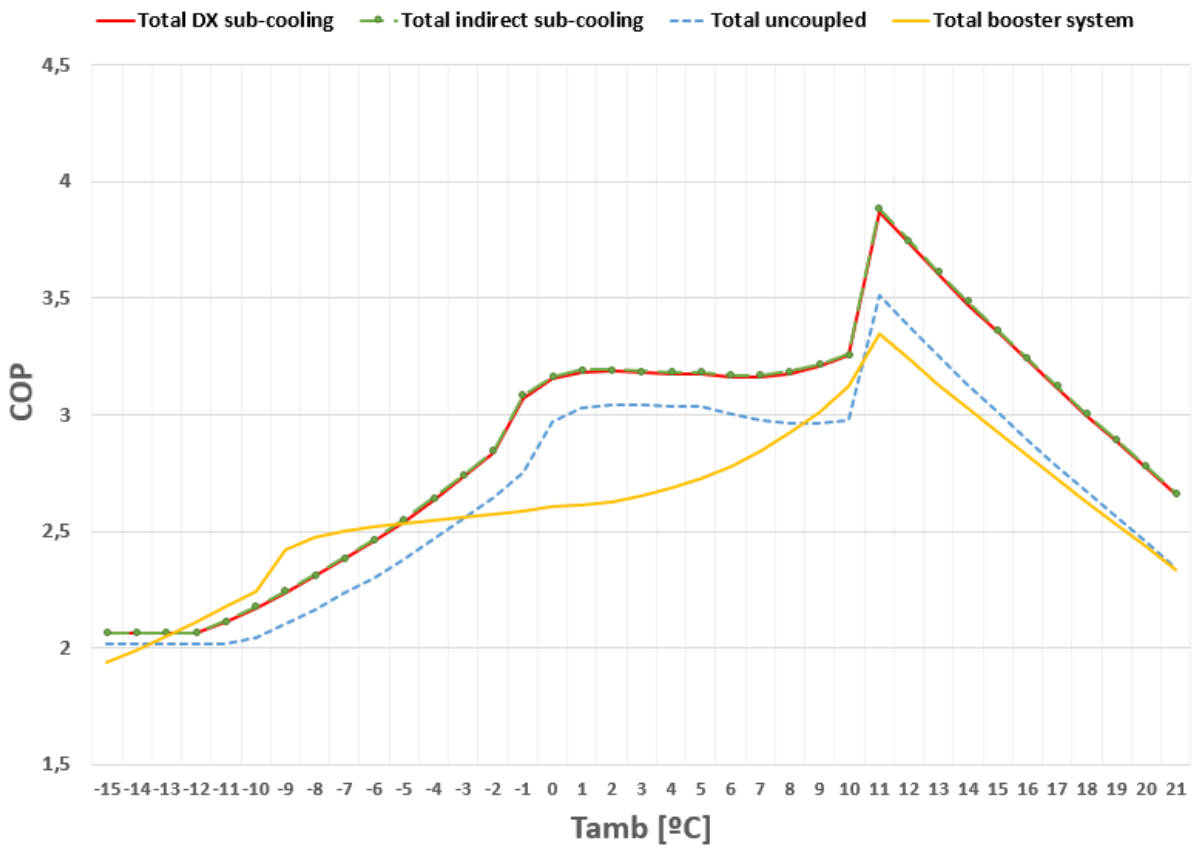

Fig. 21 Comparison graph for total COP between the system solutions with heat recovery

The results for the energy consumption yearly are shown in **Fig. 22**. Implementing the heat recovery control system, energy consumption is higher than the system solution in floating condensing mode. However, producing this heat with the CO2 system is cheaper than using other conventional heating methods. Further calculations about the economic analysis are presented in section 4.3.

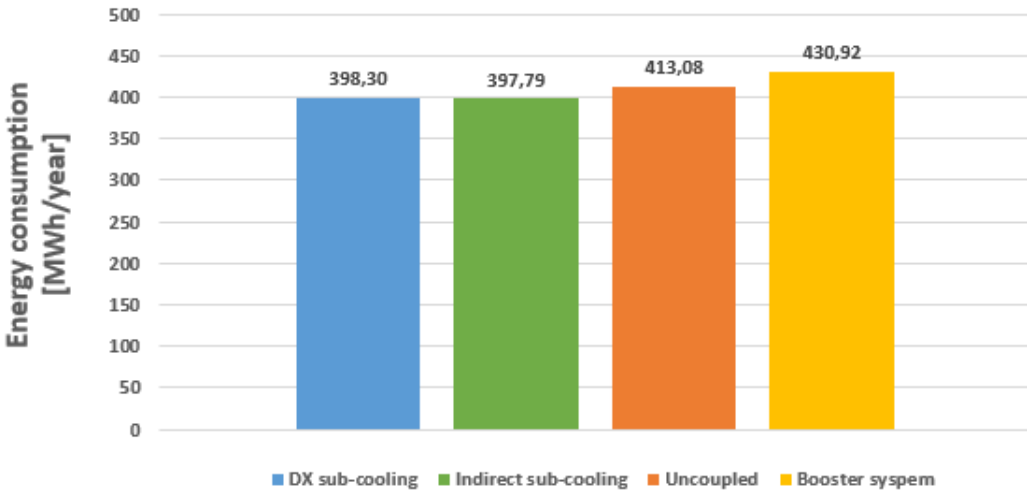

Fig. 22 Comparison chart of energy consumption for the system solutions with heat recovery [MWh/year].

These differences compared to the SotA booster system with heat recovery also implemented are shown in percentage in the **Fig. 23**. The proportion of saving remains with a similar pattern to the one presented before.

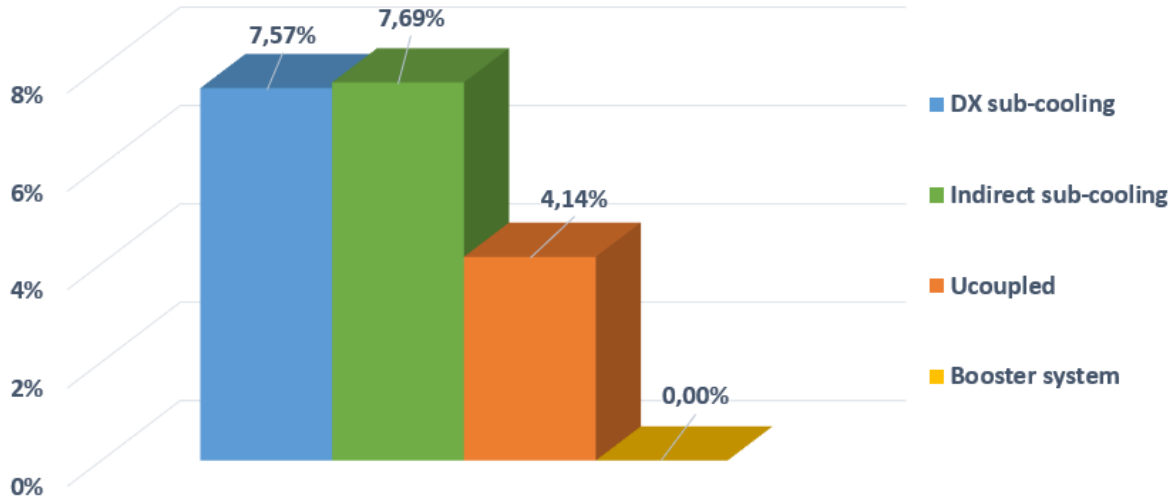

Fig. 23 Comparison chart of energy savings for the system solutions with heat recovery [%].

4.2 Discharge pressure and Temperature at the exit of the gas cooler

In this section the values of the discharge pressure and temperature at the exit of the gas cooler are discuss. These results determine in which conditions does the system perform and gives a better understanding of the temperature and pressure levels reached.

The temperature at the exit of the gas cooler follows a three-step pattern **Fig. 24**. From higher temperatures until 0 ºC the Tcg exit decreases linearly, once this temperature is reached, the curve now stabilizes at a temperature of 5 ºC. This temperature will remain until the discharge pressure does not reach its optimal maximum **Fig. 24**. Once this Pgc,opt,max is reached, the Tgc,out will increase maintaining maximum pressure until it meets the maximum temperature reachable defined by the inlet air from the gas cooler (30 ºC) plus the approach temperature defined (5 K). When these conditions are meet, the system is no longer capable of producing more heat efficiently, then if the heat load is not satisfied, other sources of heat will be needed.

As a result of this calculations, it is found that neither of the three system solution can supply enough heat to satisfy the total heat load demanded in winter mode. The maximum heat recoverable reaches its peak at 148.7 kW, while at temperatures lower than -12ºC the heating load is greater than 150 kW **Fig**. **3**. It is important to acknowledge that temperatures lower than -12 ºC represents less than 1% of the total temperatures hourly reached during the year, therefore the systems are capable to supply the need during almost the total heating season. Nevertheless, the booster system is capable of supplying this requirement, because these conditions are not reached for this system as can be seen in **Fig. 24**. The economical difference between the booster system and the standard is studied in the section 4.3.

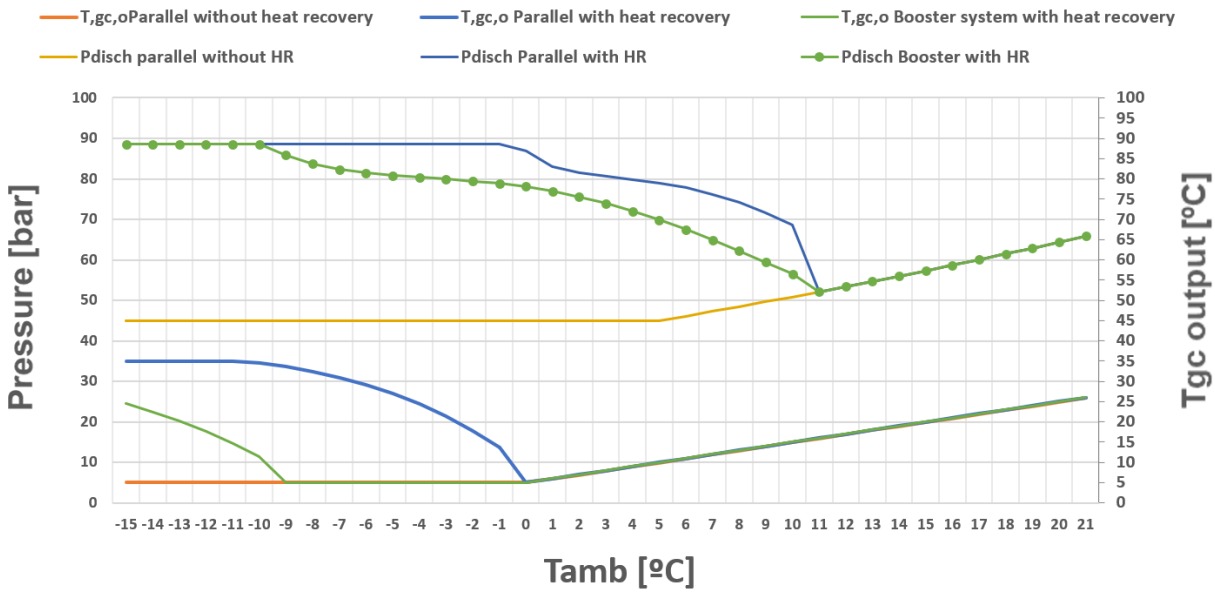

Fig. 24 Gas cooler exit temperature and Discharge pressure vs. ambient temperature plot for the different system solutions.

4.3 Economic study

To give a better understanding of the difference between solutions and systems, an economic study is performed. It is assumed an electricity price of 0.1€/kWh and 0.05€/kWh for district heating. Two cases are considered, firstly, total cost of operation to evaluate the total cost for the different systems supplying all the heat load required. Secondly, analysing only temperatures between -15 ºC and 10 ºC, to compare the cost for producing the heat demand and purchasing it from the district heating supply line.

For the total operational cost, the energy consumed by the systems and the extra heat required for the three system solution when the system is no capable to produce enough heat are considered. The yearly costs are presented in Fig. 25 Total operation cost. As can be seen, Sub-cooling and Brine secondary cycle solution, result in a very similar total cost. Then the uncoupled parallel solution is almost 1.500€ more expensive, and finally, the booster system is the highest in the spectrum with a total of 43.000€/year. Is important to acknowledge that to perform an accurate economic study, not only operational cost should be considered, but also the investment for the installation of the systems and other variable costs such as maintenance, control, etc.

Table 1 Total operation cost

	Price	DX sub-cooling	indirect sub-cooling	Uncoupled	Booster system	
Electrical	0,1€/kWh	398295,53	397791,82	413078,48	430922,2	kWh
		39.829,55 €	39.779,18 €	41.307,85 €	43.092,22 €	
DH	0,05€/kWh	7845	7845	7845	0	kWh
		392,25 €	392,25 €	392,25 €	- €	
	TOTAL	40.221,80 €	40.171,43 €	41.700,10 €	43.092,22 €	

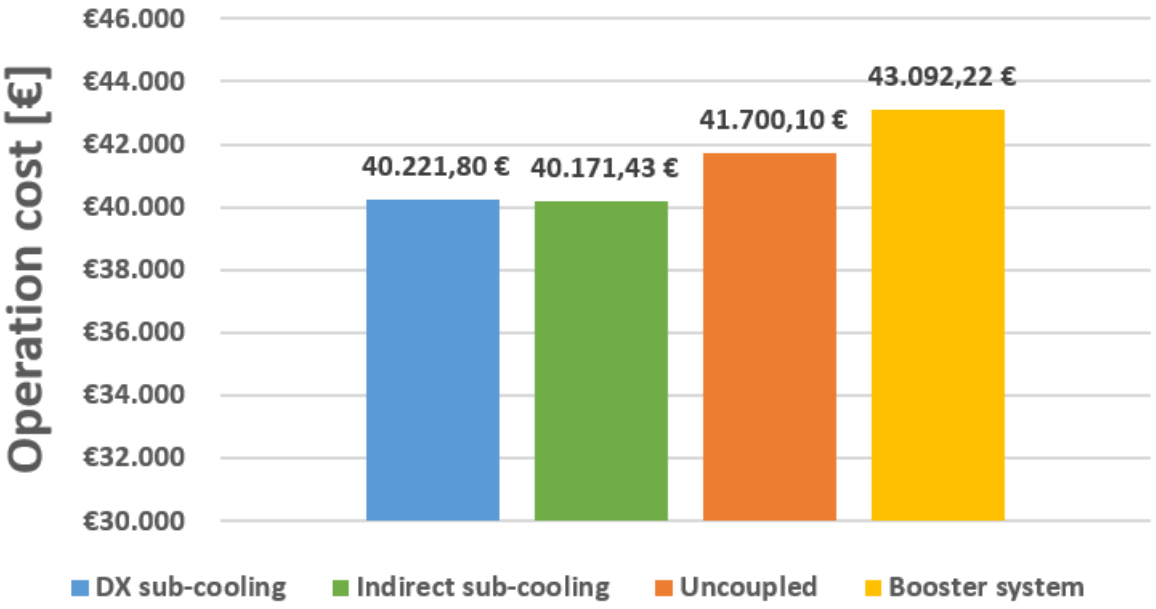

Fig. 25 Total operation cost chart for the different system solutions.

The initial investment and variable costs are too diverse depending on the project where the system will be implemented, that is unfeasible to estimate such costs. Nevertheless, knowing the percentage of savings each system can provide, gives enough information to take decisions about which option is more suitable for a project and these are shown in **Fig. 26** Total savings percentual. Even though, knowing the potential percentage savings can provide information enough to decide which system is more suitable for the project. Then **Fig. 26** is generated, comparing the savings taking the booster system as reference. Both sub-cooling and secondary brine cycle solutions give a similar result, their operational cost is 7% cheaper than the booster system, and 3% for the uncoupled solution.

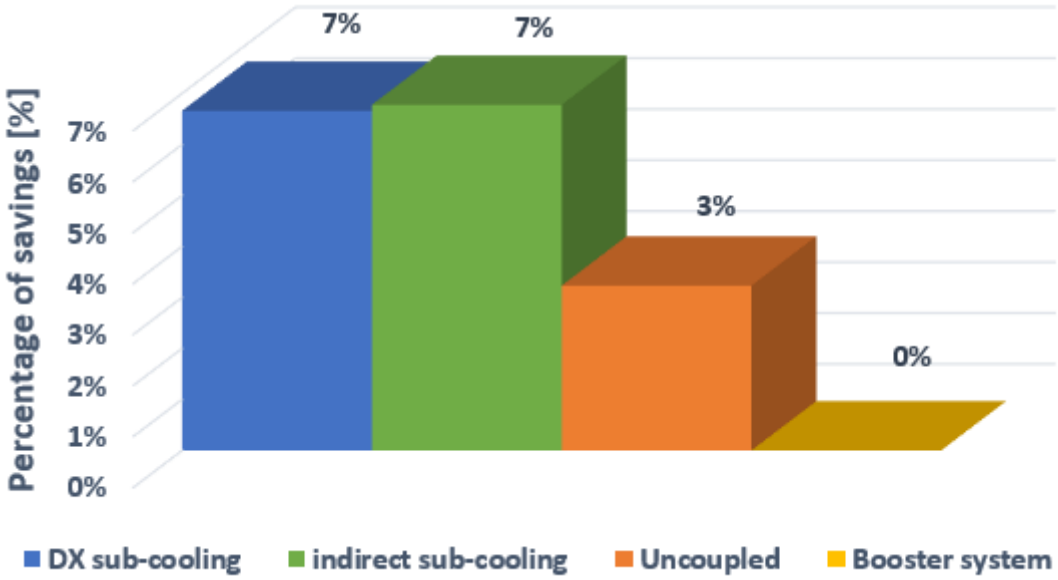

Fig. 26 Total savings percentual chart for the different system solutions.

Secondly, it is calculated the feasibility between produce or purchase the heat demanded by the sales area on the supermarket. When the heating needs are not satisfied, the extra demand is supplied by the grid. Given the small percentage yearly that this happens, this cost represents only a 1.6% of the total operation cost. The costs are broken down in **Table 2**.

Table 2 Operation cost for heating comparison.

	Price	Sub-cooling	Brine	Uncoupled	Booster system	District heating	
Electrical	0,1€/kWh	239734,53	239446,82	245733,48	259491,2	149200,3236	kWh
		23.973,45 €	23.944,68 €	24.573,35 €	25.949,12 €	14.920,03 €	
DH	0,05€/kWh	7845	7845	7845	0	400350	kWh
		392,25 €	392,25 €	392,25 €	- €	20.017,50 €	
	TOTAL	24.365,70 €	24.336,93 €	24.965,60 €	25.949,12 €	34.937,53 €	

In these cases, the total cost is lower than the total calculations because only the hours when the temperatures in the selected range are reached. Even though this distinction is applied, the solution where all the heat is purchased from the line, the total cost is 19.000€ more expensive compared to the booster system.

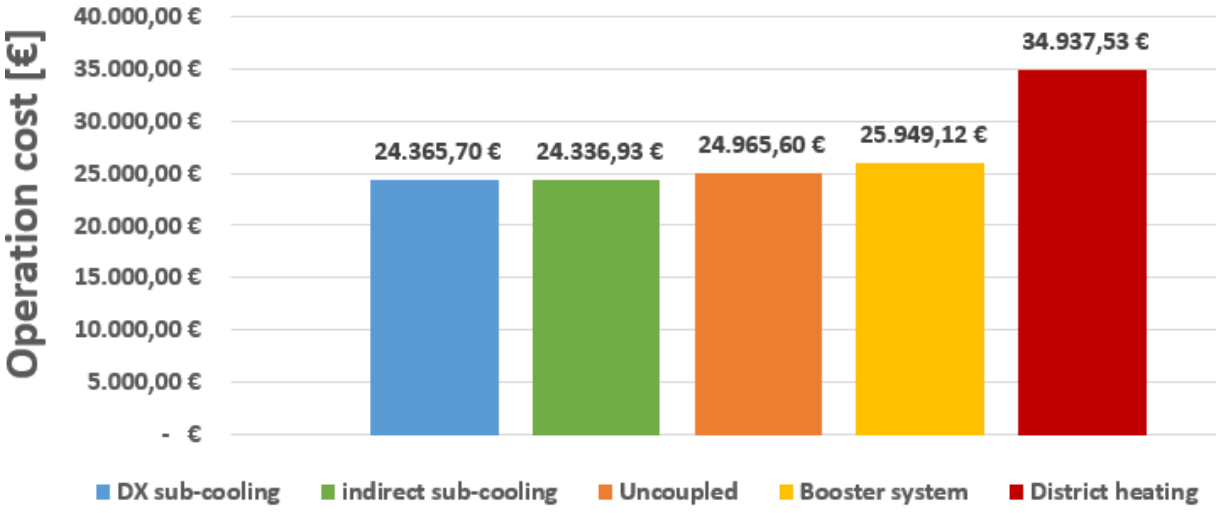

Fig. 27 Operation cost chart for heating comparison for the different system solutions.

To give a better perspective of the magnitude of savings acquired by generating heat with the system instead of buying it, **Fig. 28** is presented. As can be seen in the results, there is a potential savings of 26% for the less profitable solution, up to 30% for sub-cooling and the brine cycle configurations. It can be concluded that buying heat from the district heat grid is not economically efficient.

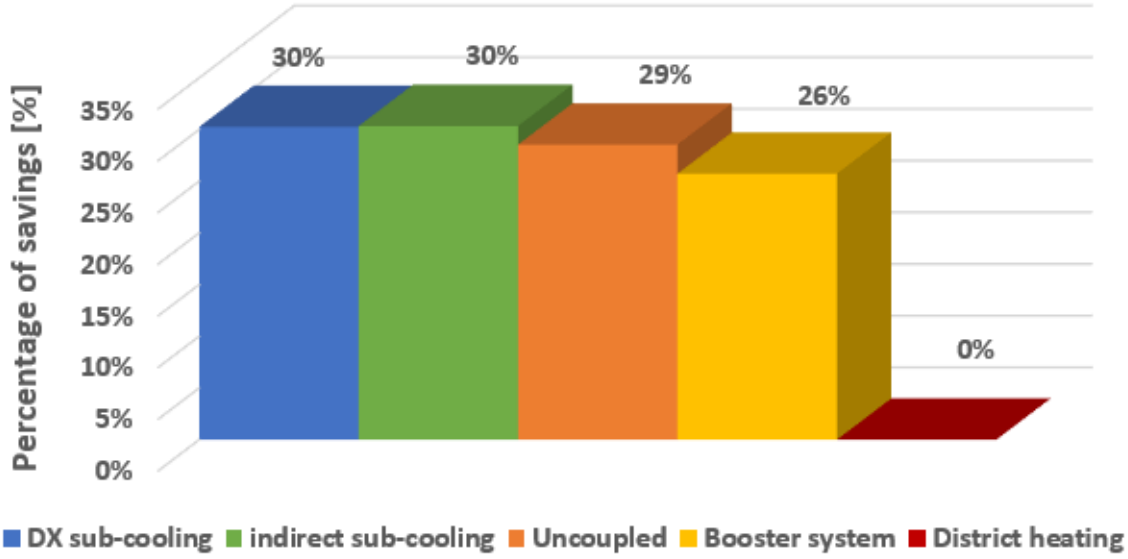

Fig. 28 Percentual savings chart for heating comparison for the different system solutions.

5 Improvements

In this section ideas for improvements that can be implemented in the parallel system to increase the efficiency are proposed. The system solution studied included improvements to increase the enthalpy difference in the evaporators, but studies show there is still room for improvement in this type of CO2 refrigeration systems. Technologies that potentially could improve these systems are explained bellow.

5.1 Ejector

Investigations in the past found, using a thermodynamic simulation, that the main cause of irreversibility in CO2 transcritical systems are caused principally in the isenthalpic expansion phase of the cycle, due to the transition from the transcritical region into a two-phase state in the refrigerant Robinson & Groll (1998). This discovery lead to further investigations about the topic and how to improve the expansion phase to reduce the level of irreversibility of the process. One solution to this problem was to introduce a ejector to decrease expansion losses and then improve the total COP Li & Groll (2005).

The configuration that Li and Groll is presented in **Fig. 29**. Introducing the ejector in the exit of the gas cooler, replacing the expansion valve, and connecting the exit to a separator which feeds the compressor. Using a throttle valve system controlled by the liquid level on the separator ensures that the mass conservation maintains with a steady-state operation. Also, connecting the separator to the evaporator feeding back part of the vapor ensures to obtain the desired quality at the evaporators inlet Li & Groll (2005).

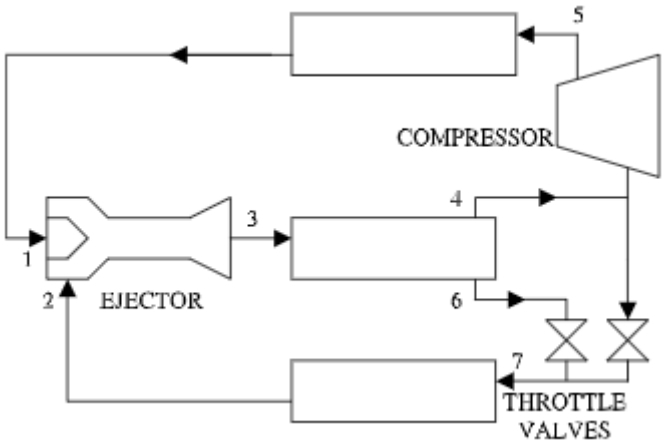

Fig. 29 Diagram for the ejector implementation example by Li and Groll (2005).

This study tested the improvement of including the ejector-expansion technology in a CO2 refrigeration system for a air-condition unit. It is important to acknowledge that the set values for these types of systems are far from the ones used in this project. Even though, this is enough to prove that this technology has the potential to improve the COP for the parallel system.

For the assumptions given in Li and Groll study, the COP improvement ranges between 7 and 18%. Further investigations should be performed to determine the COP increment that such technology could potentially improve the parallel refrigeration system.

5.2 Expander-Compressor-Unit (ECU)

As said previously in the ejector solution, the greatest opportunity to improve efficiency in this type of cycles relies in the expansion process. The expander-compressor-unit (ECU) shown in **Fig. 30**, taking advantage of the high heat sink and high pressure difference between the gas cooler exit and the evaporator entry, this unit creates mechanical work that can be used for other porpoises. In the publication made by Wenzel (2012), a test using a CO2 refrigeration system uses the work generated by the ECU run a compressor for a second stage compression process.

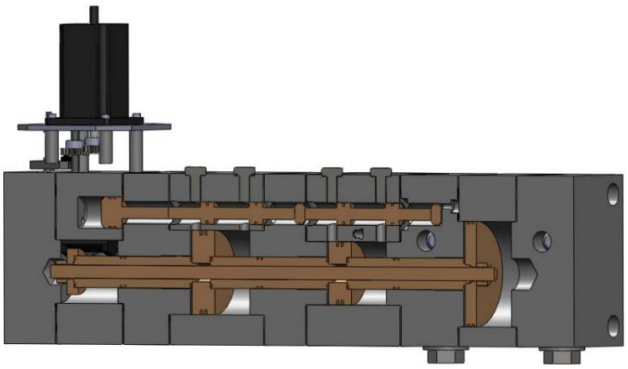

Fig. 30 Expander-Compressor-Unit (ECU) 3D render Mario WENZEL (2012).

In **Fig. 31** can be seen the diagram for the system tested by Wenzel (2012), where the expansion valve is substituted by the ECU and with a mechanical shaft torque is making the second compressor work. This technology perfectly adapts to the porpoise of the refrigeration system studied in this project because a second compression was already implemented and utilizing this unused pressure potential would decrease the power consumed by the compressors.

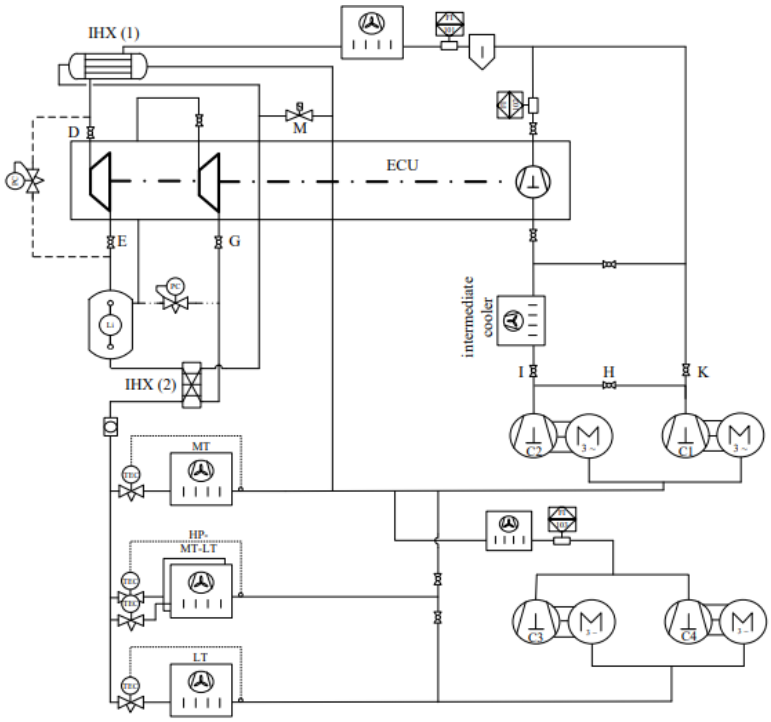

Fig. 31 Simplified flow sheet for ECU test rig Wenzel (2012).

The main issue with this type of technology is the control system because both, expansion and compression stages must be carefully monitored. But it is proven that an effective control can be achieved and make the system work efficiently. Furthermore, Wenzel's test uses similar set values as the ones described in this project ($T_{evap,MT}$ = 10 ºC and $T_{evap,LT}$ = -35 ºC Wenzel (2012)). The results of the testing carried out result in a 9.3 % COP improvement for a Booster system. similar results for the parallel system can be expected but a further study must be carried out to find the accurate improvement achievable.

6 Conclusions

Refrigerant systems are changing towards efficiency and sustainability because its crucial impact on the environment. Natural refrigerants such as CO2 are a great solution to this problem, and in its early stage of development have proven satisfactory results. SotA system are developing to be the substitute for traditional refrigeration systems. The COP achieved by the parallel trans-critical standard system proves that a market competitive solution is reached. In MT level the COP reaches a 6,8 value and LT level overcomes the 3 mark for the colder seasons of the year in flooded condensing operation.

The calculations performed in this project demonstrate the potential of the parallel system in three different configurations. Adding a direct expansion sub-cooling unit linking MT an LT loop gives similar results as using an indirect one. The main difference between these two solutions relies in the control system, being the secondary brine cycle option easier to operate because the independence of the mass flow for the sub-cooling procedure.

For all cases, implementing the heat recovery control system result in a greater efficient and economical solution to satisfy the heating load. This gives the system less dependence from the heat district grid and avoids using other less sustainable sources for this porpoise. Furthermore, using the same system for cooling and heating for the supermarket removes the necessity for two different systems, resulting in a more compact and robust solution.

The results in this thesis shows that the standard parallel CO2 refrigeration system have a better performance for the assumptions studied, with a potential energy savings of 9% in comparison with the booster system, and 7,6% when the heat recovery control system is implemented. This confirms that for the current state of development for the state-of-the art system, the parallel system with sub-cooling results in higher efficiency.

References

Accessori, E., Data, P., & Ingombri, L. (n.d.). *the Widest Co 2 Compressor Range in the Market*.

Karampour, M., & Sawalha, S. (2018). State-of-the-art integrated CO 2 refrigeration system for supermarkets : A comparative analysis. *International Journal of Refrigeration*, *86*, 239–257. https://doi.org/10.1016/j.ijrefrig.2017.11.006

Li, D., & Groll, E. A. (2005). Transcritical CO2 refrigeration cycle with ejector-expansion device. *International Journal of Refrigeration*, *28*(5), 766–773. https://doi.org/10.1016/j.ijrefrig.2004.10.008

Marimón, M. A., Arias, J., Lundqvist, P., Bruno, J. C., & Coronas, A. (2011). Integration of trigeneration in an indirect cascade refrigeration system in supermarkets. *Energy and Buildings*, *43*(6), 1427–1434. https://doi.org/10.1016/j.enbuild.2011.02.003

Mario WENZEL, U. H. (2012). COP Improvement of a CO2 Refrigeration System with an Expander-Compressor-Unit (ECU) in Subcritical and Transcritical Operation. *International Refrigeration and Air Conditioning Conference at Purdue*, 2183, Pages 1-9.

Robinson, D. M., & Groll, E. A. (1998). Efficiencies of transcritical CO2 cycles with and without an expansion turbine. *International Journal of Refrigeration*, *21*(7), 577–589. https://doi.org/10.1016/S0140-7007(98)00024-3

Sawalha, S. (2012). *Investigation of heat recovery in CO 2 trans-critical solution for supermarket refrigeration Solution au CO 2 transcritique pour le froid dans les ´ tude sur la re ´ s : E ´ cupe ´ ration de chaleur supermarche*. *6*(0).

Sawalha, S., Piscopiello, S., Karampour, M., Manickam, L., & Rogstam, J. (2017). Field measurements of supermarket refrigeration systems. Part II: Analysis of HFC refrigeration systems and comparison to CO2 trans-critical. *Applied Thermal Engineering*, *111*, 170–182. https://doi.org/10.1016/j.applthermaleng.2016.09.073

SuperSmart. (2016). *How to build a new eco-friendly supermarket*. Retrieved from http://www.r744.com/files/3supersmarthowtobuildanewecofriendlysupermarket.pdf

UNEP. (2016). *Frequently asked questions relating to the Kigali Amendment to the Montreal Protocol*. (November), 1–3.

Sweep. (2019). *6.9. Fooded evaporators*. Retrieved from https://www.swep.net/refrigerant-handbook/6.-evaporators/asas2/

Klein, S.A., 2015. Engineering Equation Solver (EES) V9, F-chart Software, Madison, USA, www.fchart.com .

Appendix 1: EES code for the parallel system

Procedure **condlimit**(t_cond_limit:t_cond)

If $(t_{cond;limit} > 10)$ Then

$t_{cond} := t_{cond;limit}$

Else

$t_{cond} := 10$

EndIf

End **condlimit**

Procedure **gascoolexit**(t_cond_check;T_gc_o_min:T_gc;o)

If $(t_{cond;check} > T_{gc;o;min})$ Then

$T_{gc;o} := t_{cond;check} - 0{,}1$

Else

$T_{gc;o} := T_{gc;o;min}$

EndIf

End **gascoolerexit**

Procedure **criticalmode**(T_condLT; T_condMT; T_amb: PcondLT;hcondLT;PcondMT;hcondMT)

If $(T_{amb} < 26)$ Then

$PcondLT := \mathbf{P}_{sat}(CarbonDioxide; T = T_{condLT})$

$hcondLT := \mathbf{h}(CarbonDioxide; T = T_{condLT}; x = 0)$

$PcondMT := \mathbf{P}_{sat}(CarbonDioxide; T = T_{condMT})$

$hcondMT := \mathbf{h}(CarbonDioxide; T = T_{condMT}; x = 0)$

Else

$PcondLT := (2{,}7 \cdot T_{condLT} - 6{,}1) \cdot 100$

$hcondLT := \mathbf{h}(CarbonDioxide; T = T_{condLT}; P = PcondLT)$

$PcondMT := (2{,}7 \cdot T_{condMT} - 6{,}1) \cdot 100$

$hcondMT := \mathbf{h}(CarbonDioxide; T = T_{condMT}; P = PcondMT)$

EndIf

End **criticalmode**

Procedure **Subcooler**(Sc_{ON};C_{ON};h_5;m_{LT};T_6;P_6;dT_C;T_8;cp;T_{12};T_{C3}:h_7;Q_{SC};h_6;m_C;Q_C;T_{C2})

If $(Sc_{ON} = 1)$ Then

$h_6 := \mathbf{h}(CarbonDioxide; T = T_6; P = P_6)$

$h_7 := h_6$

$Q_{sc} := m_{LT} \cdot (h_5 - h_6)$

$T_{C2} := 0$

$Q_C := 0$

$m_C := 0$

$T_{C3} := 0$

Else

If $(C_{ON} = 1)$ Then

$h_6 := \mathbf{h}(\text{CarbonDioxide}; T = T_6; P = P_6)$

$h_7 := h_6$

$Q_{sc} := m_{LT} \cdot (h_5 - h_6)$

$T_{C2} := T_8 + dT_C$

$Q_C := Q_{sc}$

$m_C := \dfrac{-Q_C}{cp \cdot (T_{C3} - T_{C2})}$

Else

$h_6 := h_5$

$h_7 := h_5$

$Q_{sc} := 0$

$T_{C3} := 0$

$T_{C2} := 0$

$Q_C := 0$

$m_C := 0$

EndIf

End **Subcooler**

Procedure **Temperature6**(Sc_{ON}; C_{ON}; $T_{evap;MT}$;$dT_{app;MT;SC}$;dT_C;T_{C3};$T_{gc;o}$:T_6)

If $(Sc_{ON} = 1)$ Then

$T_6 := T_{evap;MT} + dT_{app;MT;SC}$

Else

If $(C_{ON} = 1)$ Then

$T_6 := T_{C3} + dT_C$

Else

$T_6 := T_{gc;o}$

EndIf

End **Temperatur6**

Call **condlimit** $(T_{cond;Limint} : T_{cond})$

Call **gasscoolexit** $(t_{cond;check}; T_{gc;o;min}: T_{gc;o})$

Call **criticalmode** $(T_5; T_{10}; T_{amb} : T_{gc;o}; Q_{sc}; h_6; h_{10})$

Call **Subcooler** $(Sc_{ON}; C_{ON}; h_5; m_{LT}; T_6; P_6; dT_C; T_8; cp; T_{12}; T_{C3} : T_{gc;o}; Q_{sc}; h_6; h_{10}; Q_C; T_{C2})$

Call **Temperature6** $(Sc_{ON}; C_{ON}; T_{evap;MT}; dT_{app;MT;SC}; dT_C; T_{C3}; T_{gc;o} : T_6)$

$T_{cond;Limint} = T_{amb} + dT_{gc}$

$t_{cond;check} = T_{amb} + dT_{gc}$

$T_{gc;o;min} = 5$

$dT_{gc} = 5$

$dT_C = 2$

$$ISO_{per;LT} = -0{,}003 \cdot \left[\frac{P_5}{P_{evap;LT}}\right]^2 + 0{,}0354 \cdot \frac{P_5}{P_{evap;LT}} + 0{,}4676$$

$$ISO_{per;MT} = \frac{-2{,}7854 \cdot \left[\frac{P_{11}}{P_{evap;MT}}\right]^2 + 19{,}477 \cdot \frac{P_{10}}{P_{evap;MT}} + 33{,}013}{100}$$

$CD_{MT} = \mathbf{If}\ (T_{amb}; 10; 100; 100; 100 + (T_{amb} - 10) \cdot 4)$

$CD_{LT} = 35$

$HeatingDem = \mathbf{If}\ (T_{amb}; 10; 40 + (T_{amb} - 10) \cdot -5; 40; 0)$

Evaporator

$T_{evap;LT} = -32$

$SH_{evap;LT} = 10$

$P_{evap;LT} = \mathbf{P}\ (CarbonDioxide; T = T_{evap;LT}; x = 1)$

$T_1 = T_{evap;LT} + SH_{evap;LT}$

$P_1 = P_{evap;LT}$

$h_1 = \mathbf{h}\ (CarbonDioxide; P = P_1; T = T_1)$

$s_1 = \mathbf{s}\ (CarbonDioxide; P = P_1; T = T_1)$

$$m_{LT} = \frac{CD_{LT}}{h_1 - h_7}$$

$\rho_{LT} = \rho\ (CarbonDioxide; T = T_1; P = P_1)$

$$Vflow_{LT} = \frac{m_{LT}}{\rho_{LT}}$$

Compressor

$s_{2s} = s_1$

$P_2 = P_3$

$h_{2s} = \mathbf{h}(\text{CarbonDioxide}; P = P_2; s = s_{2s})$

$P_3 = \sqrt{P_1 \cdot P_5}$

$T_3 = T_5$

$h_3 = \mathbf{h}(\text{CarbonDioxide}; T = T_3; P = P_3)$

$s_3 = \mathbf{s}(\text{CarbonDioxide}; T = T_3; P = P_3)$

$P_4 = P_5$

$s_{4s} = s_3$

$h_{4s} = \mathbf{h}(\text{CarbonDioxide}; P = P_4; s = s_{4s})$

$$E_{1;2} = m_{LT} \cdot \left[\frac{h_{2s} - h_1}{ISO_{per;MT}}\right]$$

$$E_{3;4} = m_{LT} \cdot \left[\frac{h_{4s} - h_3}{ISO_{per;MT}}\right]$$

$E_{3;4;sh} = m_{LT} \cdot (h_4 - h_3)$

$E_{1;2;sh} = m_{LT} \cdot (h_2 - h_1)$

$E_{1;2;sh} = 0{,}93 \cdot E_{1;2}$

$E_{3;4;sh} = 0{,}93 \cdot E_{3;4}$

$E_{LT;2single} = E_{1;2} + E_{3;4}$

$$E_{LT} = m_{LT} \cdot \left[\frac{h_{4s} - h_1}{ISO_{per;LT}}\right]$$

$T_{HE;LTe} = 35$

$h_{HE;LTe} = \mathbf{h}(\text{CarbonDioxide}; T = T_{HE;LTe}; P = P_5)$

$Heat_{Aw;LT} = m_{LT} \cdot (h_4 - h_{HE;LTe})$

$T_5 = T_{cond}$

$T_{between5and6} = T_{gc;o}$

$h_{between5and6} = \mathbf{h}(\text{CarbonDioxide}; T = T_{between5and6}; P = P_5)$

$SC_{cond;LT} = 5$

$SC_{LT} = T_{between5and6} - T_6$

$dT_{app;MT;SC} = 5$

$P_6 = P_5$

$s_6 = \mathbf{s}(\text{CarbonDioxide}; P = P_6; T = T_6)$

E.Valve

$Sc_{ON} = 1$

$C_{ON} = 0$

$P_7 = P_1$

Secondary cycle

$T_{C3} = T_{12} + dT_C$

Evaporator

$T_{evap;MT} = -8$

$SH_{evap;MT} = 10$

$P_{evap;MT} = \mathbf{P}(\text{CarbonDioxide}; T = T_{evap;MT}; x = 1)$

$T_8 = T_{evap;MT} + SH_{evap;MT}$

$P_8 = P_{evap;MT}$

$h_8 = \mathbf{h}(\text{CarbonDioxide}; T = T_8; P = P_8)$

$s_8 = \mathbf{s}(\text{CarbonDioxide}; T = T_8; P = P_8)$

Compressor

$P_9 = P_{10}$

$s_{9s} = s_8$

$h_{9s} = \mathbf{h}(\text{CarbonDioxide}; P = P_9; s = s_{9s})$

$E_{MT;shaft} = 0{,}93 \cdot E_{MT}$

$E_{MT;shaft} = (m_{MT} + m_{SC}) \cdot (h_9 - h_8)$

$$E_{MT} = (m_{MT} + m_{SC}) \cdot \left[\frac{h_{9s} - h_8}{ISO_{per;MT}}\right]$$

$T_{HE;MTe} = 35$

$h_{HE;MTe} = \mathbf{h}(\text{CarbonDioxide}; T = T_{HE;MTe}; P = P_9)$

$Heat_{Av;MT} = m_{MT} \cdot (h_9 - h_{HE;MTe})$

$T_{10} = T_{cond}$

$P_{11} = P_{10}$

$T_{11} = T_{gc;o}$

$h_{11} = \mathbf{h}(\text{CarbonDioxide}; T = T_{11}; P = P_{11})$

$P_{12} = P_8$

$h_{12} = h_{11}$

$T_{12} = \mathbf{T}(\text{CarbonDioxide}; P = P_{12}; h = h_{12})$

$$m_{MT} = \frac{CD_{MT}}{h_8 - h_{12}}$$

$$m_{SC} = \frac{Q_{sc}}{h_8 - h_{12}}$$

$m_{MTgc} = m_{MT} + m_{SC}$

$HE_{LT} = 0$

$$Q_{HR;MT} = \textbf{If}\ (T_{amb};\ 10;\ Heat_{Av;MT};\ Heat_{Av;MT};\ 0)$$

$$Q_{HR;LT} = \textbf{If}\ (HE_{LT};\ 1;\ 0;\ Heat_{Av;LT};\ 0)$$

$$Q_{extraNeed} = HeatingDem - Q_{HR;MT} + Q_{HR;LT}$$

$$Q_{LT} = m_{LT} \cdot (h_1 - h_7)$$

$$Q_{MT} = m_{MT} \cdot (h_8 - h_{12})$$

$$Hours = 0$$

$$Energy_{tot;double} = (E_{MT} + E_{LT}) \cdot Hours$$

$$Energy_{tot;2single} = (E_{MT} + E_{LT;2single}) \cdot Hours$$

$$Energy_{MT;double} = E_{MT} \cdot Hours$$

$$Energy_{MT;2single} = E_{MT} \cdot Hours$$

$$Energy_{LT;double} = E_{LT} \cdot Hours$$

$$Energy_{LT;2single} = E_{LT;2single} \cdot Hours$$

$$COP_{LT;2single} = \frac{CD_{LT}}{E_{LT;2single}}$$

$$COP_{MT} = \frac{CD_{MT} + Q_{sc}}{E_{MT}}$$

$$COP_{tot} = \frac{CD_{LT} + CD_{MT}}{E_{LT} + E_{MT}}$$

$$COP_{tot;2single} = \frac{CD_{LT} + CD_{MT}}{E_{LT;2single} + E_{MT}}$$

Appendix 2: Results from Dorin for the Compression correlation

Data collected from Dorin software for the semi-hermetic double staged compressor CD2S1200 in the working conditions for the parallel system

T_ev	P_disch	T_gc_e	T_cond	Q_2	E_el	P_ev	PR	eff_tot
[C]	[kPa]	[C]	[C]	[kW]	[kW]	[kPa]		
-40	0	0	0,5	7,56	3,84	1005	3,52	0,4788
-40	0	0	5	7,19	4,11	1005	3,95	0,4939
-40	0	0	10	6,76	4,41	1005	4,48	0,5081
-40	0	0	15	6,3	4,74	1005	5,06	0,5165
-40	0	0	20	5,79	5,07	1005	5,70	0,5232
-40	0	0	25	5,19	5,41	1005	6,41	0,5277
-35	0	0	15	7,7	4,98	1202	4,23	0,5215
-35	0	0	20	7,08	5,36	1202	4,77	0,5293
-35	0	0	25	6,36	5,74	1202	5,35	0,5365
-30	0	0	15	9,33	5,19	1428	3,56	0,5217
-30	0	0	20	8,59	5,6	1428	4,01	0,5341
-30	0	0	25	7,72	6,03	1428	4,51	0,5429
-25	0	0	20	10,34	5,83	1683	3,41	0,5319
-25	0	0	25	9,3	12,8	1683	3,82	0,5436
-20	0	0	25	11,12	6,55	1970	3,27	0,5401
-40	75	30	0	4,63	5,91	1005	7,47	0,5268
-40	90	30	0	5,07	6,42	1005	8,96	0,538
-35	75	30	0	5,69	6,26	1202	6,24	0,542
-35	90	30	0	6,24	6,81	1202	7,49	0,5584
-35	100	40	0	4,86	7,34	1202	8,32	0,548
-30	75	30	0	6,92	6,62	1428	5,25	0,5506
-30	90	30	0	7,6	7,25	1428	6,30	0,57
-30	100	40	0	5,94	7,78	1428	7,00	0,5655
-30	110	45	0	5,36	8,27	1428	7,70	0,561
-25	75	30	0	8,35	6,95	1683	4,46	0,5564
-25	90	30	0	9,17	7,67	1683	5,35	0,5781
-25	100	40	0	7,18	8,29	1683	5,94	0,5727
-25	110	45	0	6,49	8,76	1683	6,54	0,5747
-20	75	30	0	9,99	14	1970	3,81	0,5562
-20	90	30	0	10,97	8,05	1970	4,57	0,5834
-20	100	40	0	9,6	8,78	1970	5,08	0,5766
-20	110	45	0	7,79	9,33	1970	5,59	0,5792
-15	75	30	0	11,85	7,56	2291	3,27	0,5503
-15	90	40	0	13,02	8,43	2291	3,93	0,5824
-15	100	45	0	10,21	9,23	2291	4,37	0,5775
-15	110	30	0	9,25	9,89	2291	4,80	0,5787
-10	90	30	0	15,33	8,78	2649	3,40	0,576
-10	100	40	0	12,02	9,69	2649	3,78	0,5717
-10	110	45	0	10,89	10,44	2649	4,15	0,5737

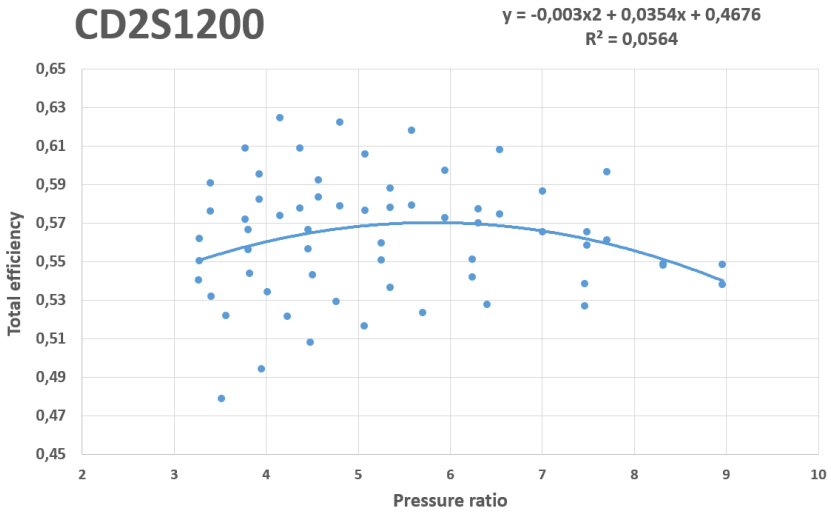

Test with exit temperature of the gas cooler set at 25 °C.

T_ev	P_disch	T_gc_e	T_cond	Q_2	E_el	P_ev	PR	eff_tot
[C]	[kPa]	[C]	[C]	[kW]	[kW]	[kPa]		
-40	75	25	0	5,44	5,81	1005	7,47	0,5385
-40	90	25	0	5,6	6,32	1005	8,96	0,5483
-35	75	25	0	6,68	6,19	1202	6,24	0,5509
-35	90	25	0	6,88	6,74	1202	7,49	0,5654
-35	100	25	0	6,69	7,09	1202	8,32	0,5486
-30	75	25	0	8,12	6,55	1428	5,25	0,5596
-30	90	25	0	8,37	7,17	1428	6,30	0,5772
-30	100	25	0	8,47	7,53	1428	7,00	0,5865
-30	110	25	0	8,55	7,84	1428	7,70	0,5964
-25	75	25	0	9,78	6,86	1683	4,46	0,5663
-25	90	25	0	10,09	7,55	1683	5,35	0,5879
-25	100	25	0	10,22	7,98	1683	5,94	0,5973
-25	110	25	0	10,32	8,34	1683	6,54	0,6079
-20	75	25	0	11,69	7,17	1970	3,81	0,5663
-20	90	25	0	12,07	7,94	1970	4,57	0,5922
-20	100	25	0	12,23	8,39	1970	5,08	0,6059
-20	110	25	0	12,36	8,8	1970	5,585	0,618
-15	75	25	0	13,87	7,44	2291	3,274	0,5617
-15	90	25	0	14,33	8,26	2291	3,929	0,5953
-15	100	25	0	14,53	8,8	2291	4,365	0,6089
-15	110	25	0	14,68	9,26	2291	4,802	0,6224
-10	90	25	0	16,88	8,58	2649	3,398	0,5906
-10	100	25	0	17,12	9,15	2649	3,776	0,6087
-10	110	25	0	17,3	7,66	2649	4,153	0,6245

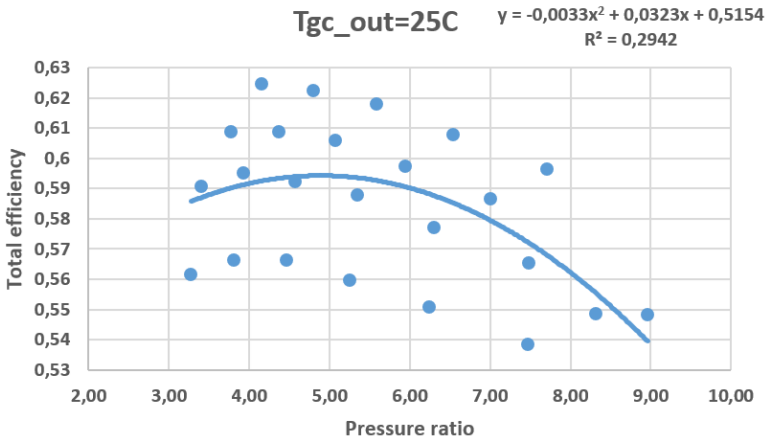
Tgc_out=25C
y = -0,0033x² + 0,0323x + 0,5154
R² = 0,2942
Total efficiency
0,63
0,62
0,61
0,6
0,59
0,58
0,57
0,56
0,55
0,54
0,53
2,00
3,00
4,00
5,00
6,00
7,00
8,00
9,00
10,00
Pressure ratio